NATIONAL ADVISORY COMMITTEE FOR AERONAUTICS

WARTIME REPORT

ORIGINALLY ISSUED

December 1945 as Advance Restricted Report L5J05

EFFECTS OF WING AND NACELLE MODIFICATIONS ON

DRAG AND WAKE CHARACTERISTICS OF A

BOMBER-TYPE AIRPLANE MODEL

By Robert H. Neely, Richard W. Fairbanks, and D. William Conner

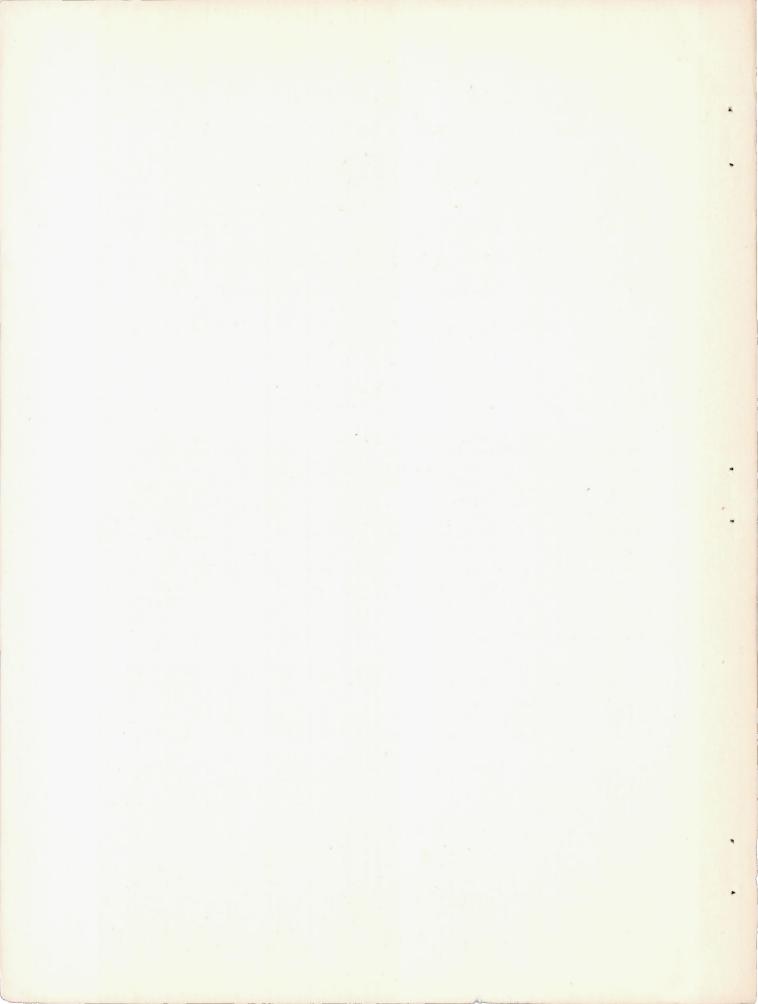
Langley Memorial Aeronautical Laboratory Langley Field, Va.

PROPERTY OF JET PROPULSION LABORATORY LIBRARY
CALIFORNIA INSTITUTE OF TECHNOLOGY



WASHINGTON

NACA WARTIME REPORTS are reprints of papers originally issued to provide rapid distribution of advance research results to an authorized group requiring them for the war effort. They were previously held under a security status but are now unclassified. Some of these reports were not technically edited. All have been reproduced without change in order to expedite general distribution.



NATIONAL ADVISORY COMMITTEE FOR AERONAUTICS

ADVANCE RESTRICTED REPORT

EFFECTS OF WING AND NACELLE MODIFICATIONS ON

DRAG AND WAKE CHARACTERISTICS OF A

BOMBER-TYPE AIRPLANE MODEL

By Robert H. Neely, Richard W. Fairbanks and D. William Conner

SUMMARY

An investigation of a model of a large four-engine bomber was conducted in the Langley 19-foot pressure tunnel to determine the effects of several wing and nacelle modifications on drag characteristics and airflow characteristics at the tail. Leading-edge gloves, trailing-edge extensions, and modified nacelle afterbodies were tested individually and in combination. The effects of the various modifications were determined by force tests, tuft observations, and turbulence surveys in the region of the tail. Tests were made with fixed and natural transition on the wing and with propellers operating and propellers off. Most of the tests were conducted at a Reynolds number of approximately 2.6 × 106.

The results indicated that application of certain of the modifications provided worth-while improvements in the characteristics of the model. The flow over the wing and flaps was improved, the drag was reduced, and the turbulence in the region of the tail was reduced.

Trailing-edge extensions were the most effective individual modification in improving the flow over the wing with wing flaps neutral, cowl and intercooler flaps closed. Modified nacelle afterbodies were the most effective individual modification in reducing drag with either fixed or natural transition on the wing; however, trailing-edge extensions were slightly more effective with fixed transition. Combinations of either leadingor trailing-edge extensions and modified afterbodies were more effective than either modification alone. With cowl and intercooler flaps open, trailing-edge extensions with modified afterbodies provided substantial improvement in

flow and drag characteristics. With wing flaps deflected, enclosing the flap behind the inboard nacelle within an extended afterbody or cutting the flaps at the nacelle appeared to be the most promising methods of improving the flow over the flaps and the tail. Although the results of hot-wire-anemometer surveys were not conclusive in regard to buffeting characteristics, the modifications did reduce the turbulence at the tail with wing flaps both neutral and deflected. The modifications, as a rule, were favorable to maximum lift. Appreciable reductions in longitudinal stability of the model were caused by addition of leading-edge gloves and trailing-edge extensions.

INTRODUCTION

Separation of flow over a wing increases the drag and has, in a number of instances, caused tail buffeting because of the irregular nature of the flow at the tail. Several wing and nacelle modifications, designed with a view to improving the flow over the wing, were tested on a model of a large four-engine bomber to determine the effects on drag characteristics and air-flow characteristics at the tail. Leading-edge gloves, wing trailing-edge extensions, and modified nacelle afterbodies were tested. The characteristics of the basic and modified model were determined by tuft observations, force measurements, and measurements of turbulence and dynamic pressure in the vicinity of the tail. Turbulence was measured by means of a hot-wire anemometer. The hot-wireanemometer equipment was furnished by the California Institute of Technology and was operated under the direction of Dr. Hans W. Liepmann of its staff. The investigation was conducted in the Langley 19-foot pressure tunnel.

SYMBOLS

The coefficients and symbols used herein are defined as follows:

C_L gross lift coefficient (L/qS)

ACImax increment of maximum lift coefficient

c_D	drag coefficient corrected for jet-boundary interference (D/qS)
C _m	gross pitching-moment coefficient (M/qSc)
c_{D_i}	induced-drag coefficient $(c_L^2/\pi A)$
c_{D_p}	parasite-drag coefficient $(c_D - c_{D_i})$
Δc_{D_p}	increment of parasite-drag coefficient
Tc	thrust disk-loading coefficient for one propeller $\left(T_{\rm e}/\rho V^2 D^2\right)$
$\sqrt{v^2}$	root-mean-square value of the deviations, per- pendicular to wind axis, of instantaneous local velocity from its mean value
U	mean value of instantaneous local velocity along wind axis
q _t	local dynamic pressure at tail
q	free-stream dynamic pressure $\left(\frac{1}{2}\rho V^2\right)$
α	angle of attack of wing corrected for jet- boundary interference
$\delta_{\mathbf{f}}$	wing-flap deflection measured from neutral flap position
R	Reynolds number $(\rho V \overline{c}/\mu)$
where	
L	lift
D	drag; propeller diameter
M	pitching moment about center of gravity
Te	effective thrust of one propeller
S	wing area (22.219 sq ft)

mean aerodynamic chord (1.444 ft)

A geometric aspect ratio $\left(\frac{b^2}{S} = 12.8\right)$

b wing span (16.875 ft)

V velocity in free stream

ρ mass density of air

μ coefficient of viscosity

MODEL

The general arrangement of the model is shown in figures 1 and 2. The model was of wood and metal construction and was finished with lacquer. Pertinent dimensions are given in table I.

The wing had Davis airfoil sections, 22.9 percent thick at the root and 9.3 percent thick at the tip. The maximum camber was approximately 3.4 percent of the chord at the root section and 1.4 percent at the tip. The location of the maximum camber was constant across the span at 31.5 percent of the local chord. The geometric aspect ratio of the wing was 12.8 and the taper ratio was 3.077:1.

The horizontal tail had no movable elevator. The vertical tail was off during all the tests.

The installation of the cowl flaps and intercooler exit flaps is shown in figure 3 for their deflected positions. The cowl flaps extended from the top of the cowling to a point slightly below the nacelle center line. The intercooler cooling-air exits were located on the upper surface of the wing.

STANDARD CONFIGURATION

The standard nacelle afterbodies (afterbody 1) are shown in figures 3 and 4 with wing flaps neutral. No part of the nacelle afterbody is on the upper surface of

the wing near the trailing edge. The extreme end of the standard afterbodies was attached to the lower surface of the wing flaps and deflected with the flaps, as shown in figure 5. The wing flaps were of the Fowler type and consisted of inboard and outboard sections. Ordinates for the inboard section are given in table II. At the inboard nacelle, the nose of the flap was 2.4 percent wing chord ahead of and 2.9 percent wing chord below the trailing edge of the wing.

MODIFICATIONS

In an attempt to delay separation of air flow on the wing in the cruise condition, the original wing chord was extended in order to reduce the peak pressures and adverse pressure gradients. Leading-edge gloves (figs. 6 and 7) were built to NACA 64-series ordinates modified to fair into the original Davis airfoil section. The gloves extended the wing chord 10 percent between the fuselage and the inboard nacelle and tapered to the original leading edge at the outboard nacelle. Because these gloves were added to the original wing, a perfect contour could not be formed where the gloves faired into the wing.

The trailing-edge extension was a thin metal strip attached to the flaps and deflected down 11° from the lower surface of the flaps. The extensions were deflected down 1° to 2° from the wing chord lines. The installation of the extensions is shown in figure 7. Extensions of two different spans and three different chords were tested. Extensions attached only to the inboard flaps are designated 0.3 span, and extensions attached to both inboard and outboard flaps are designated 0.6 span. The chords were $1\frac{1}{2}$, $2\frac{1}{1}$, and 3 inches. Unless otherwise specified, the term "trailing-edge extensions" designates the $1\frac{1}{2}$ -inch-chord extensions attached to both the inboard and outboard flaps.

The installation of the various modified nacelle afterbodies with wing flaps neutral is illustrated in figures 8 to 10. Drawings of the modified nacelle afterbodies are given in figures 11 to 13. Afterbodies 2 and 3, shown in figure 8, were attached to the inboard nacelles only and differed mainly from the standard afterbody in that they had a fairing on the upper surface

of the wing. Afterbody 4 (figs. 9 and 12) was a beaver-tail afterbody with a small fairing on the upper surface of the wing. Afterbody 5, shown in figures 10 and 13, was faired on the upper surface of the wing forward to the intercooler air exit. The lower part was extended in order to obtain a better afterbody shape.

The installation of the deflected flaps with inboard nacelle afterbodies 4 and 5 is shown in figures 14 and 15, respectively. With afterbodies 4, tests were made with the flaps cut out below the afterbody as shown in figure 14 and also with the flaps not cut and extending below the afterbody. Inboard afterbodies 5 enveloped the center part of the deflected flaps, and the flap-nacelle juncture was faired with plasticine as shown in figure 15. The tips of the modified afterbodies did not deflect with the flaps.

A double slotted, or vaned, flap (fig. 16) was tested in an attempt to improve the air flow over the flap. The outside contour and the installation of the flap and vane combination were the same as for the original Fowler flap. The ordinates for the double slotted flap are given in table II.

APPARATUS AND TESTS

Tests of the model were made for two basic conditions:

- (1) Cruise condition wing flaps neutral, cowl and intercooler flaps closed
- (2) Landing condition wing flaps deflected 40°, landing gear down, cowl and intercooler flaps closed

For the cruise condition, a few tests were also made to determine characteristics with cowl and intercooler flaps open.

For the cruise condition, tests were made with the model in the standard configuration and with leading-edge gloves, trailing-edge extensions, and modified nacelle afterbodies. For the landing condition, tests were made with the model in the standard configuration and with modified inboard afterbodies and modified inboard flaps.

The cowl flaps in the open position were deflected 10°. When the intercooler flaps were opened, the exit gap was increased 7/16 inch, which corresponds to the maximum deflection of the intercooler flaps. The air flow through the nacelle was adjusted, with the model at an angle of attack of 5°, to provide a pressure drop of approximately 0.75q through the cowling with cowl flaps open and a pressure drop of approximately 0.67q through the intercooler ducts with exit flaps closed.

For a flap deflection of 40°, the main landing gear was down; however, no provision was made for simulating open landing-gear doors. For flap deflections of 0° and 10°, the landing gear was removed. Most of the tests were made with the horizontal tail off. The vertical tail was off for all tests.

Power conditions were simulated by matching the thrust coefficients of the model and airplane at each lift coefficient. The variation of thrust coefficient with lift coefficient for sea-level power conditions is presented in figure 17. The thrust coefficients for 0.4 normal rated power at sea level correspond closely to those for cruising power (0.6 normal rated power) at 25,000 feet. The propeller blade angle at 0.75 radius was 30°.

It was believed that transition from laminar to turbulent flow on the airplane wing would occur at approximately the location of the front spar. In an attempt to make the results of the model tests more representative of flight conditions, most of the tests were made with the transition fixed at a chordwise station corresponding to the spar location. The transition was fixed by placing a strip of 60-grain carborundum on the upper and lower surfaces at the 10-percent-chord station of the original wing section. The width of the strip between the fuse-lage and the outboard nacelles was approximately 3/8 inch and tapered to approximately 1/4 inch at the tips.

The character of the flow over the wing and the nacelle afterbodies was determined by observing the behavior of tufts, which were attached to both the upper and lower surfaces of the wing and nacelle afterbodies. No tufts were placed ahead of the 20-percent-chord station of the wing. These tests were generally made with fixed transition and with propellers operating at 0.4 normal rated power; however, a few tests were made with natural transition and with propellers off.

Force and moment characteristics were measured by a six-component automatically recording balance system. Lift and drag were measured for all configurations. The effects of leading-edge gloves and trailing-edge extensions on the longitudinal stability characteristics were determined with the horizontal tail on (elevator neutral) for several power conditions.

Measurements of the air-stream turbulence were made at several spanwise stations along the elevator hinge line by means of a hot-wire anemometer. The basic principles of operation of this instrument are described in reference 1. The turbulence measurements were supplemented by measurements of the local dynamic pressures at the tail obtained from surveys with a rake of six pitot-static tubes. All surveys were made with fixed transition and with the propellers operating at 0.4 normal rated power.

All tests were made with the air in the tunnel compressed to an absolute pressure of approximately 35 pounds per square inch ($\rho \approx 0.00558$ slug/cu ft). Most of the tests were made at a Reynolds number of approximately 2.6 \times 10⁶ and a Mach number of 0.12; however, a few tests were made at a Reynolds number of 3.9 \times 10⁶ and a Mach number of 0.18.

RESULTS AND DISCUSSION

The results of the investigation are discussed from the standpoint of (1) flow over the wing and flap, (2) flow at the tail, (3) drag and lift, and (4) longitudinal stability. The characteristics of the standard model and the effect of the various modifications are shown for the cruise and landing conditions.

Jet-boundary corrections have been added to the angle of attack, drag coefficient, and the vertical position of the survey points with respect to the elevator hinge line as follows:

 $\Delta \alpha = 0.654c_{L}$ $\Delta c_{D} = 0.0106c_{L}^{2}$ $\Delta z = -0.13c_{L}$

where $\Delta\alpha$ is in degrees, Δz is in inches, and z is the vertical position of the survey points with respect to the elevator hinge line. No corrections have been applied to the data for the effects of model-support tare and interference or for air-stream misalinement.

FLOW CHARACTERISTICS AT THE WING

The results of tuft observations that show the character of the flow over the wing, flaps, and nacelles are given.

Cruise Condition

The stall progressions of the model in the original and modified configurations with wing flaps neutral are given in figures 18 to 22 for cowl and intercooler flaps closed. The values of lift coefficient at which separation first occurred on the wing are given in table III. Diagrams showing the flow over the wing at a lift coefficient of approximately 0.8 are presented in figure 23. Stall progressions for the model with cowl and intercooler flaps open are given in figure 24. The propellers were operating at 0.4 normal rated power and the transition was fixed at 10 percent wing chord except for two tests of the standard model. Diagrams are presented to show the effect of power and the effect of removing the transition strip on the wing.

Standard configuration .- With cowl and intercooler flaps closed, propellers operating at 0.4 normal rated power, and transition fixed, the initial stall on the wing occurred at a lift coefficient of about 0.63 with the model in the standard or original configuration (fig. 18(a)). The initial separation occurred on the rear part of the wing to the left of each nacelle. The flow over the wing directly behind each nacelle was rough but not separated for most angles of attack. With natural transition (fig. 18(b)) the stall patterns were about the same as with fixed transition but the initial separation occurred at a lift coefficient of about 0.91. With propellers off and transition fixed, the initial separation occurred at about the same lift coefficient as with the propellers operating, but at higher lift coefficients the area directly behind the inboard nacelles was stalled (fig. 18(c)).

Separated flow like that indicated in figure 18 produces an increase in drag and could cause buffeting. The purpose of the modifications was to delay this separation and to cause a general improvement in flow through the cruising range (c_L = 0.6 to 0.9). A substantial improvement in flow over the wing was obtained, as shown in figure 25(a), by deflecting the wing flaps 10°. The drag, however, was increased.

Chord extensions. - Chord extensions delayed the initial separation and improved the flow over the wing at higher lift coefficients.

Leading-edge gloves (fig. 19(a)) delayed the initial separation to a lift coefficient 0.12 higher than for the standard model. About the same improvement was realized with the 1^{\perp} -inch-chord 0.3-span trailing-edge extensions. The 0.6-span trailing-edge extensions were the most effective individual modification in improving the flow over the wing. The 1-inch-chord 0.6-span trailing-edge extensions (fig. 19(c)) delayed the initial separation to a lift coefficient 0.21 higher than for the standard model. More improvement resulted from the 2-inch-chord 0.6-span extensions. Subsequent tests, however, were made with the $1\frac{1}{2}$ -inch-chord 0.6-span trailing-edge extensions because the greater improvement in flow with the 2-inch extensions did not seem sufficient to warrant the additional structural changes necessary to the airplane. In evaluating the improvement due to either leading-edge or trailing-edge extensions in terms of the increase in lift coefficient at which separation first occurred on the wing, it should be noted that the gain in lift coefficient was partly due to added wing area.

Modified nacelle afterbodies. - Modified nacelle afterbodies caused only a slight delay in the initial separation but improved the flow over the wing. This improvement is shown for afterbodies 2 and 3 by comparing figure 20 with figure 18(a) and for afterbodies 4 and 5 by comparing figures 21(a), 21(b), 22(a), and 22(b) with figures 19(a) and 19(c). Afterbodies 4 and 5 appear to be most effective. No flow separation occurred on the lower surface of either the standard or modified nacelles.

Combinations of chord extensions and modified nacelle afterbodies .- Chord extensions, either leading edge or trailing edge, in combination with modified nacelle afterbodies were more effective in delaying separation and in improving the flow over the wing than were chord extensions or afterbodies alone. The combinations of leading-edge gloves with afterbodies 4 and leading-edge gloves with afterbodies 5 (figs. 21(a) and 22(a)) delayed the initial separation to a lift coefficient approximately 0.16 higher than for the standard model. With trailing-edge extensions in combination with either afterbodies 4 or 5 (figs. 21(b) and 22(b)), the initial separation occurred at a lift coefficient of about 0.91, which is approximately 0.28 higher than for the standard model. As shown in figure 21(c), a greater improvement in flow was obtained with a combination of leading-edge gloves, trailing-edge extensions, and afterbodies 4. Separation on the inner wing sections was delayed to a lift coefficient of over 1.0. A similar combination with afterbodies 5 was only slightly more effective than the combination of trailing-edge extensions with afterbodies 5.

Cowl and intercooler flaps open. With the model in the standard configuration, opening the cowl and intercooler flaps caused separation of the flow over the wing directly behind them at all lift coefficients (fig. 24(a)). The addition of trailing-edge extensions reduced the extent of the stalled area, as shown in figure 24(b). With afterbodies 4 and trailing-edge extensions on the model (fig. 24(c)), the initial separation behind the open intercooler flaps was delayed until a lift coefficient of about 0.55 had been reached. With inboard afterbodies 5 and trailing-edge extensions on the model, no separation occurred behind the open intercooler flaps of the inboard nacelles (fig. 24(d)).

Landing Condition

Stall characteristics of the standard and modified model with wing flaps deflected are shown in figures 25 to 27. For these configurations the propellers were operating at 0.4 normal rated power, the transition was fixed, and the cowl and intercooler flaps were closed.

Standard configuration. - With the standard configuration and flaps deflected hoo (fig. 25(b)), the initial stall on the wing occurred ahead of the ailerons and was

followed by separation between the nacelles. For all angles of attack and all flap deflections, separation occurred on the part of the flaps blanketed by the nacelles. The flow over the lower surface of the nacelle and the part of the afterbody that deflected with the flap was not separated. (See fig. 26(a).) Removing the afterbody tips from the standard model did not improve the flow over the flaps. It was thought that separated flow over the inboard flaps combined with irregular flow created by the afterbody tips would probably contribute most to any tail buffeting. Modifications for the landing condition were therefore directed toward improving the air flow at the inboard nacelles.

Modifications .- With double slotted inboard flaps deflected 400 (fig. 26(b)), the flow over the right flap was not separated but the left flap was stalled, as was the standard flap. From tests made with the afterbody tips removed and with power off, the separation over the double slotted inboard flaps at 0.4 normal rated power appeared to be caused by the afterbody tip, which deflected with the flap, and the dissymmetry appeared to be associated with the rotation of the slipstream. When the standard flaps were continuous and were deflected through afterbodies 4 (fig. 26(c)), the lower part of the afterbody and the surface of the flap below the afterbody were stalled at all angles of attack. With the flaps cut out at inboard afterbodies 4, as shown in figure 14, no stall occurred on the flap or nacelle (fig. 26(d)). The same flow existed with trailing-edge extensions on the flaps. With the standard flaps deflected within afterbodies 5 (fig. 26(e)), the flow over the flaps and afterbodies was not separated at any angle of attack. Adding trailing-edge extensions had little effect on the flow if the extensions were cut out below the nacelles (fig. 26(f)).

The most promising methods of those investigated for improving the flow over the flap were enclosing the flap rear of the inboard nacelle within afterbody 5 or cutting the flap at the nacelle. Trailing-edge extensions and modified afterbodies, to a lesser extent, delayed separation on the inner wing panels and thus aggravated the tendency toward early tip stalling indicated by stall studies of the standard model. This effect could be minimized by reducing the wing-flap deflection.

FLOW CHARACTERISTICS AT THE TAIL

The results of turbulence surveys at the tail are presented in figures 28 to 31 for the standard model and for several modifications. Diagrams showing the flow characteristics over the wing for conditions at which surveys were made are given in figure 32. The turbulence data are presented as the variation of root-mean-square value of the vertical velocity deviations with vertical distance for several spanwise stations. Axial velocity deviations were of the same order of magnitude as vertical velocity deviations. Maximum values of the velocity deviation are several times the root-mean-square values. The vertical velocity deviations may be interpreted as angle-of-attack changes; for example, a value

of $\sqrt{v^2}/U$ of 0.04 is equivalent to a root-mean-square angle deviation of slightly over 20.

Buffeting tendencies are difficult to evaluate quantitatively because the root-mean-square deviation indicates neither the large fluctuations that may occur nor the frequency. Both of these factors play an important role in determining buffeting characteristics. The main value of the data presented is the indication of the effects of the modifications on the turbulent wake. The curves indicate the normal wake of the wing and nacelles by an increase of turbulence. Beyond this main turbulent wake, there are small peaks that define the edge of the slipstream.

The variations of local dynamic pressure with vertical distance for the standard model are indicated in figures 33 to 35. The curves show increases in dynamic pressure due to the slipstream and depressions due to wing or nacelle wake. The point at which the maximum depression occurs has been assumed to be the center of the wake. The variations of wake-center position with lift coefficient are given in figures 36 and 37 for the standard and modified models. Except for displacement, the modifications changed the profile of the dynamic-pressure wake very little.

The vertical position of the peak values of turbulence agree closely with the position of the dynamic-pressure wake centers. The vertical extent of the main turbulent wake is roughly the same as that for the

dynamic-pressure wake. A comparison of the turbulence and dynamic-pressure-survey data indicates that only a slight amount of turbulence is produced by the slipstream; the greater part of the turbulence is produced by the wake of the wing and nacelles.

Cruise Condition

Standard configuration. For the standard model with cowl and intercooler flaps closed (fig. 28), the largest turbulent wake and the maximum turbulence occurred at stations 13 inches right and 27 inches left of the fuselage center line, which are behind stalled parts of the

wing (fig. 32). The maximum value of $\sqrt{v^2}/U$ obtained with cowl and intercooler flaps closed was 0.04. As shown in figures 28 and 33, the variations of turbulence and dynamic pressure are different on the left and right sides of the fuselage center line. The growth of turbulence on the left side from the high-speed condition through the cruise condition is illustrated in figure 29. At stations to the right and left of the inboard nacelle (13 in. and 27 in. from fuselage center line) the turbulence increased with increasing angle of attack. Directly behind the nacelle, the turbulence decreased slightly as the angle of attack increased from 4.4° to 7.6°. With increasing angle of attack, the wake centers moved up in relation to the elevator hinge line (figs. 29 and 36).

Combinations of chord extensions and modified nacelle afterbodies .- The effects of modifications, in general, were to reduce the extent and magnitude of the turbulence and to displace the whole turbulent wake downward. As shown in figure 28, the greatest reduction in turbulence was obtained with afterbodies 4 in combination with trailing-edge extensions. The combination of afterbodies 5, trailing-edge extensions, and leading-edge gloves was somewhat less effective; and the combination of afterbodies 5 and trailing-edge extensions was the least effective in reducing turbulence. The greatest reductions in turbulence were obtained at stations 13 inches right and 27 inches left and right of the fuselage center line. These reductions are apparently due to modifications delaying separation on the wing at these stations. At the station directly behind the nacelles (20 in.), afterbodies 4 caused a definite reduction in

turbulence whereas afterbodies 5 caused little change. The downward displacement of the wake due to modifications would be greater than shown in figure 28 if the data were compared at the same lift coefficient. (See fig. 36.)

Cowl and intercooler flaps open. - Comparison of figures 28 and 30 shows that opening the cowl and intercooler flaps caused large increases in the turbulence at the tail both with the standard model and with afterbodies 5 and trailing-edge extensions. The magnitude and extent of the velocity fluctuations were, however, much lower for the model with afterbodies 5 and trailing-edge extensions.

Landing Condition

The results of surveys for the landing condition are given in figure 31 for a spanwise station behind the inboard nacelle. With both the standard and modified

models, the maximum value of $\sqrt{v^2}/U$ occurred below the elevator hinge line.

With the flaps deflected within afterbodies 5, the turbulence was less than for the standard model. With flaps continuous and deflected through afterbodies 4, slightly greater turbulence was obtained than for the standard model. The increased turbulence was evidently due to the stall that occurred on the flap and lower part of the afterbody (fig. 26(c)). With the flaps cut out below the nacelle as shown in figure 14, the turbulence would probably be less than for the standard model.

DRAG AND LIFT CHARACTERISTICS

The variations of the parasite-drag coefficient with lift coefficient for the standard and modified model are shown in figures 38 to 45. The lift, drag, and pitching-moment characteristics for the cruise and landing conditions are given in figures 46 to 52. Table III gives the numerical values of the drag changes due to modifications at several lift coefficients and the increments of maximum lift coefficients due to the modifications

obtained in the cruising condition. The data have not been corrected for support tares or air-stream misaline-ment and therefore should not be considered as absolute values nor should the shape of the curves be considered correct. It is believed, however, that the changes in drag and lift due to modifications would not be materially affected by the application of such corrections.

Cruise Condition

Inasmuch as flight Reynolds numbers are much greater than that at which the tests were conducted, the interpretation of the drag reductions due to the modifications is difficult, particularly in the range where separation occurs. The value of drag reductions obtained at a given lift coefficient of the model may not be in agreement with reductions that would be obtained from tests of the full-scale airplane. The results of the model tests, however, are believed to be indicative of the results that would be obtained from installation of the modifications on the airplane.

Figure 38 presents the data obtained from runs made near the beginning, middle, and end of the investigation with fixed and natural transition. The displacement of the test points gives an indication of how closely test conditions (primarily model surface condition) could be duplicated. Fixing the transition at 10 percent wing chord increased the drag coefficient at all values of lift coefficient and also decreased the lift coefficient at which the rapid increase in drag occurs.

The effect of Reynolds number on drag characteristics with transition fixed is shown in figure 39. The drag for each model configuration was lower at all lifts at a Reynolds number of 3.9×10^6 than at a Reynolds number of 2.6×10^6 , and the knee in the drag curves occurred at higher lifts with the higher Reynolds number.

Chord extensions. - The effect of span and chord of the trailing-edge extensions in reducing drag is shown

in figure 40. At a lift coefficient of 0.7, reductions with 0.3-span and 0.6-span extensions were approximately in the ratio of 3:4. The $2\frac{1}{4}$ -inch-chord extensions reduced the drag somewhat more than the $1\frac{1}{2}$ -inch extensions. No further reduction was realized by increasing the chord to 3 inches. Subsequent tests were made with the 0.6-span $1\frac{1}{2}$ -inch-chord trailing-edge extensions.

Changes in drag caused by trailing-edge extensions and leading-edge gloves were dependent upon the type of transition. The $1\frac{1}{2}$ -inch-chord 0.6-span trailing-edge extensions reduced the drag coefficient of the model by 0.0038 with transition fixed at a lift coefficient of 0.7 (fig. 41(a)). With natural transition (fig. 41(b)), the trailing-edge extensions increased the drag 0.0003 at a lift coefficient of 0.7 but at lift coefficients above 0.8 appreciable reductions were obtained. Leadingedge gloves reduced the drag coefficient by 0.0028 at a lift coefficient of 0.7 with fixed transition and by 0.0012 with natural transition (fig. 41). Because of the imperfect contour formed where the gloves faired into the wing, the results obtained with the wing modified in this manner are probably not so good as would be obtained if the wing were built to the revised dimensions.

Modified nacelle afterbodies .- All modified inboard nacelle afterbodies reduced the drag of the model at cruising lifts (fig. 42) but had little effect at low lifts. The order of increasing effectiveness was afterbodies 2, 3, 4, and 5. Modified afterbodies on all four nacelles reduced the drag at all lift coefficients. Four afterbodies 4 reduced the drag coefficient of the model by 0.0034 with fixed transition and 0.0017 with natural transition at a lift coefficient of 0.7 (fig. 43). Four afterbodies 5 (fig. 44) were somewhat less effective in reducing the drag than four afterbodies 4. Modified nacelle afterbodies were the most effective individual modifications in reducing drag when considering both fixed and natural transition on the wing; however, trailing-edge extensions were slightly more effective with fixed transition.

Propellers-off stall studies of the standard model (fig. 18(c)) show that at a lift coefficient of about 0.7

the flow behind the inboard nacelles was separated but the flow behind the outboard nacelles was smooth. These studies and a consideration of the shape of the drag curves indicate that the modified inboard afterbodies reduce the drag by delaying separation on the wing, whereas the modified outboard afterbodies reduce the drag by improving the afterbody form. This explanation probably accounts for the differences between the effectiveness of the inboard and outboard afterbody modifications.

Combinations of chord extensions and modified nacelle afterbodies.— The combination of chord extensions and modified nacelle afterbodies generally was more effective in reducing drag than either modification alone. Some of the more effective combinations with the drag-coefficient reductions at $C_{\rm L}=0.7$ are as follows:

Modification	Fixed transition	Natural transition
Four afterbodies 4 and trailing- edge extensions	0.0045	0.0015
Four afterbodies 5 and trailing- edge extensions	0.0038	0.0005
Four afterbodies 5 and leading- edge gloves	0.0046	0.0015
Four afterbodies 5, leading-edge gloves, and trailing-edge extensions	0.0048	0.0017

There appears to be no advantage in combining leadingedge gloves with afterbodies 4 for reducing drag.

All modifications increased the maximum lift coefficient of the model with either fixed or natural transition, and most of the modifications increased the slope of the lift curve.

Cowl and intercooler flaps open. - With the model in the standard configuration, opening the cowl and

intercooler flaps caused a large increase in drag. (Compare figs. 45 and 38.) The resulting high drag coefficient was decreased 0.0072 at a lift coefficient of 0.7 by the addition of inboard afterbodies 5 and trailing-edge extensions or four afterbodies 4 and trailing-edge extensions (fig. 45). It should be noted that these modifications reduced the drag coefficient approximately 0.0040 with cowl and intercooler flaps closed.

Landing Condition

The lift characteristics for the standard and modified models with wing flaps deflected 40° are presented in figure 52. With transition fixed and propellers off, the same maximum lift coefficient was obtained with double slotted inboard flaps or with standard flaps deflected within afterbodies 5 as was obtained with the model in the standard configuration.

In order to eliminate flow separation that occurred on the flaps and the rear part of afterbodies 4, part of the inboard flaps were cut away. This change resulted in a reduction of about 0.1 in the maximum lift coefficient. An additional reduction would result if the outboard flaps were cut. With flaps deflected through either afterbodies 4 or 5, the addition of trailing-edge extensions increased the maximum lift coefficient by about 0.2; the resulting lift coefficient was greater in both cases than for the standard model.

LONGITUDINAL STABILITY CHARACTERISTICS

Pitching-moment curves for the standard and modified model with propellers removed and horizontal tail off are presented in figures 46 to 51. Power-on pitching-moment curves with horizontal tail on and off are presented in figures 53 to 55. No corrections have been applied to the pitching moments but the results presented indicate the effect of the various modifications. With tail on, the large differences in trim and the fact that large parts of the curves are considerably out of trim make an accurate evaluation of stability changes difficult. Moment curves for several elevator or stabilizer settings would be required.

As indicated by changes in the slopes of the pitching-moment curves, leading-edge gloves and trailing-edge extensions caused appreciable reductions in longitudinal stability.

Cruise Condition

With wing flaps neutral and the horizontal tail on (fig. 53), the pitching-moment curves show that the model with chord extensions and modified afterbodies was less stable than the standard model for all power conditions. Up to a lift coefficient of 0.6, the combination of trailing-edge extensions and inboard afterbodies 5 changed the moment-curve slope dCm/dCT approximately 0.04 to 0.06 from the standard configuration. The combination of leading-edge gloves, trailing-edge extensions, and afterbodies 5 changed the slope approximately 0.08 to 0.10 from the standard configuration. Above a lift coefficient of 0.6, the modifications were more destabilizing, probably because the delayed separation on the inner wing panel results in increased downwash. A satisfactory compromise between the adverse stability changes and flow and drag improvements due to trailing-edge extensions could probably be obtained with an extension having a smaller chord than those tested.

Landing Condition

With wing flaps deflected, horizontal tail on, and propellers operating at 0.4 normal rated power (fig. 54(b)), the slope of the pitching-moment curve was approximately 0.04 less negative (model less stable) with the combination of trailing-edge extensions and afterbodies 5 on the model. With leading-edge gloves, trailing-edge extensions, and afterbodies 5 on the model, the slope of the moment curve was 0.07 less negative than with the model in the standard configuration. With propellers operating at zero thrust (fig. 54(a)), only a slight change in the slope of the moment curve was caused by either modification. The adverse effects on stability could be minimized by reducing the flap deflection.

CONCLUSIONS

From an investigation of a model of a four-engine bomber-type airplane that was made to determine effects of wing and nacelle modifications on drag and air flow at the tail, the following results were shown:

- l. Worth-while improvements in the characteristics of the model were obtained with certain modifications. The improvements were indicated on the basis of improved flow over the wing and deflected flaps, reduced turbulence in the region of the tail, and reduced drag.
- 2. Trailing-edge extensions were the most effective individual modification in improving the flow over the wing with wing flaps neutral, cowl and intercooler flaps closed. Modified nacelle afterbodies were the most effective individual modification in reducing drag with either fixed or natural transition on the wing; however, trailing-edge extensions were slightly more effective with fixed transition. Four afterbodies 4 (a beaver-tail type) alone were superior to four afterbodies 5 (an extended conventional afterbody) alone in reducing drag. Combinations of either leading- or trailing-edge extensions and modified afterbodies were more effective in delaying separation and reducing the drag than either modification alone.
- 3. With the model in the standard configuration, opening the cowl and intercooler exit flaps caused separation on the wing behind the intercooler air exit, increased the drag considerably, and increased the turbulence at the tail. These conditions were greatly improved by adding modified nacelle afterbodies and trailing-edge extensions.
- 4. With wing flaps deflected, enclosing the flap behind the inboard nacelle within nacelle afterbody 5 or cutting the flaps at the nacelle appear to be the most promising methods of improving the flow over the flaps and reducing the turbulence at the tail.
- 5. Although the results of turbulence surveys made with a hot-wire anemometer do not indicate definitely that buffeting would occur with the standard model or that the modifications would eliminate buffeting, the modifications did reduce the turbulence at the tail with wing flaps either neutral or deflected.

- 6. Appreciable reductions in the longitudinal stability of the model were caused by leading-edge gloves and trailing-edge extensions. In the landing condition, chord extensions also aggravated the tendency toward early tip stalling obtained with the standard model.
- 7. All modifications increased the maximum lift with wing flaps neutral and gave a maximum lift equal to or greater than that for the standard model with wing flaps deflected except when the inboard flaps were cut out below afterbodies 4.

Langley Memorial Aeronautical Laboratory
National Advisory Committee for Aeronautics
Langley Field, Va.

REFERENCE

1. Dryden, H. L., and Kuethe, A. M.: The Measurement of Fluctuations of Air Speed by the Hot-Wire Anemometer. NACA Rep. No. 320, 1929.

TABLE I

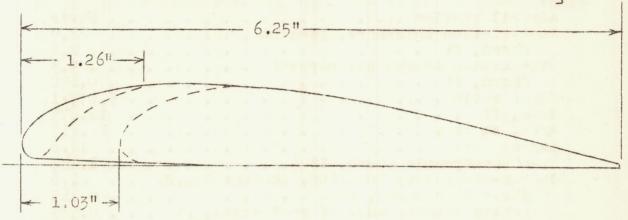
GENERAL SPECIFICATIONS OF MODEL

to the seal of the season of t
Wing:
Airfoil section Davis Root-section thickness, percent
Chord. ft
Chord, ft
Chord, ft
Taper ratio
Span, ft
Area, sq ft
Aspect ratio
Mean aerodynamic chord, ft
Above root chord, ft
Behind leading edge of root chord, ft 0.525
Incidence (with respect to fuselage
center line), deg 3.0
Geometric twist, deg
Fuselage:
Over-all length, ft
Maximum frontal area, sq ft
Manahan i olivat al va, by 10
Nacelles:
Frontal area (each), sq ft 0.450
Incidence (with respect to wing chord), deg3.0
77
Horizontal tail:
Area, sq ft
Incidence (with respect to fuselage
center line), deg1.0
center line), deg1.0 Elevator hinge-line location (fuselage
horizontal)
Horizontal distance rear of leading edge of
root chord, ft
root chord, ft 0.031
Propellers:
Number
Number Diameter, ft
Blades
Blade design Curtiss Wright 1016-16

TABLE II

ORDINATES FOR FOWLER AND DOUBLE SLOTTED FLAPS

Stations and ordinates given in inches and are measured from leading edge and reference line of Fowler flap



-	F	owler fla	p	Double	e slotted	flap
	Station	Upper surface	Lower surface		Vane	
	0	0.196	0.196	Station		ower rface
	.078 .156 .312 .469 .625 .937	.364 .442 .554 .632 .688 .769	.078 .062 .0148 .014 .0140 .0314 .026	0.156 .28 .l:1 .53 .78 1.03 1.26		.06 .12 .30 .46 .64 .75
	1.875	.821	.014	No	se of fla	p
	3.125 3.750 4.375	.760 .653 .522	0	Station	Upper surface	Lower surface
A distance outside spirit of some spirits or some outside out the spirits	5.000 5.625 6.25	.366 .220 .040	0	1.03 1.11 1.19 1.34	0.20 .38 .45	0.20
-	L.E.	radius:	0.125	1.50	.70	
		ONAL ADVI		1.97 2.28 2.50	.78 .82 .82	

TABLE III EFFECT OF MODIFICATIONS ON DRAG, STALL, AND LIFT IN THE CRUISE CONDITION $\delta_f = 0^\circ$; cowl and intercooler flaps closed; R $\approx 2,600,000$

Modifications	ΔC _{Dp} with fixed transition		ACDp with natural transition		C _L at first stall, O _s ! normal rated power, fixed transition	ΔCI _{max} with propellers off	
	$c_{\rm L} = 0.14$	$c_L = 0.7$	c _L = 0.7	c _L = 0.9	(a)	Fixed transition	Natural transition (b)
None					0.63		
CTwo afterbodies 2	0	-0.0005			0.64		
CTwo afterbodies 3	0	-0.0010			0.65		
CTwo afterbodies 4	0	-0.0015			***************		
CTwo afterbodies 5	0	-0.0021					
Four afterbodies 4	-0.0008	-0.0034	-0.0017	-0.0029		0.09	0.11
Four afterbodies 5	-0.0006	-0.0027	-0.0011	-0.0021		0.07	0.10
L.E. gloves	-0.0003	-0.0028	-0.0012	0.0019	0.75	0.05	
L.E. gloves, four afterbodies 4	-0.0006	-0.0042	-0.0004	0	d _{0.80}	0.15	
L.E. gloves, four afterbodies 5	-0.0010	-0.0046	-0.0015	-0.0016	40.79	0.15	44400000
T.E. extensions	-0.0003	-0.0038	0.0003	-0.0010	0.84	0.12	0.14
T.E. extensions, four afterbodies 4	-0.0008	-0.0045	-0.0015	-0.0029	0.91	0.17	0.20
T.E. extensions, four afterbodies 5	-0.0002	-0.0038	-0.0005	-0.0017	d _{0.91}	0.19	0.25
L.E. gloves, T.E. extensions			-0.0004	0			
L.E. gloves, four afterbodies 4, T.E. extensions	-0.0009	-0.0051	-0.0007	-0.0011	a _{1.04}	0.24	
L.E. gloves, four afterbodies 5, T.E. extensions	-0.0006	-0.0048	-0.0017	-0.0025	d _{0.90}	0.28	

aLift coefficient given is that at which separation of flow first occurred on wing. bFor configurations with L.E. gloves, see lift curves.

CWhen two modified nacelle afterbodies were tested, they were fitted to inboard nacelles only.

dstall studies with modified inboard afterbodies only.

INDEX TO FIGURES

a. Illustrative Figures

Figure Material presented						
1 2	Three-view drawing of model					
2	Model mounted in test section					
3	Photograph, standard nacelle afterbodies, of = 00					
L	Drawing, standard nacelle afterbodies					
5	Photograph, standard nacelle afterbodies, & = 400					
345	Drawing, L.E. gloves					
7	Photograph, L.E. gloves and T.E. extensions					
3	Photograph, nacelle afterbodies 2 and 3					
9	Photograph, nacelle afterbodies 4, of = 00					
10	Photograph, nacelle afterbodies 5, of = 00					
11	Drawing, nacelle afterbodies 3					
12	Drawing, nacelle afterbodies 4					
13	Drawing, nacelle afterbodies 5					
1/4	Photograph, nacelle afterbodies 4, of = 400					
12 13 14 15	Photograph, nacelle afterbodies 5, of = 400					
16	Photograph, double slotted flap					
17	Calculated thrust coefficients for B-32 airplane					

b. Stalling Characteristics; 0.4 Normal Rated Power; Transition Fixed

Figure	Configuration	ôf (deg)	Cowl and inter- cooler flaps
18(a)	Standard model	0	Closed
*18(b)		0	Do.
b18(c)		0	Do.
19	Chord extensions	0	Do.
20	Modified inboard afterbodies	Q.	Do.
21	Inboard afterbodies 4 and chord extensions Inboard afterbodies 5 and chord	0	Do.
22	extensions	0	Do.
23	Comparison of stall patterns at $C_L \approx 0.8$	0	Do.
24	Standard and modified model	0	Open
25(a)	Standard model	10	Closed
25(b)		40	Do.
26	Standard and modified model (flow over inboard afterbodies and flaps) Modified model (flow over wing)	40	Do.

aNatural transition. bPropellers off.

INDEX TO FIGURES - Concluded

c. Tail-Survey Data; O.4 Normal Rated Power; Transition Fixed

Figure	Material presented	Form of data	8f (deg)	Cowl and inter-
28 29 30 31 32	Standard and modified model, $\alpha = 7.6^{\circ}$ and 8.7° Effect of angle of attack Standard and modified model, $\alpha = 7.5^{\circ}$ Standard and modified model, $\alpha = 12.7^{\circ}$ Stall patterns for survey conditions	u against vertical distance	0000	Closed Do. Open Closed
33 34 35 36 37	Standard model	qt against vertical distance Vertical distance against CL	{ 0 0 0 0 0 0 0 0 0 0 0 0 0 0 0 0 0 0 0	Closed Open Closed Do. Open

d. Aerodynamic Characteristics with Propellers Off

Figure	Material presented	Form of data	ôg (deg)	Cowl and inter- cooler flaps	Transition
38	Several runs with standard model	CDp against CL	0	Closed	Fixed and natural
39 40 41	Effect of Reynolds number T.E. extensions Standard afterbodies with chord	do	0	do	Pixed Do.
42	extensions Effect of various nacelle	do	0	do	natural
43	afterbodies Afterbodies with chord	do	0	do	Fixed and
44	extensions Afterbodies 5 with chord	do	0	do	natural
45	extensions Effect of modifications with cowl and intercooler flaps	40.0	0	do	Do.
	open	do	0	Open	Fixed
46	Effect of transition	CD, a, Cm against CL	0	Closed	Fixed and natural
47	T.E. extensions Standard afterbodies with chord	do	0	00	Fixed and
49	extensions Afterbodies 4 with cherd	do	0	do	natural
50	extensions Afterbodies 5 with chord	do	0	do	Do.
	extensions	do	0	do	Do.
51	Effect of modifications with cowl and intercooler flaps open	do	0	Open	Fixed
52	Effect of modifications on lift	C _{T.} against a	40	Closed	Do.

e. Longitudinal Stability Characteristics; Transition Fixed

Figure	Configuration	ôf (deg)	Cowl and inter- cooler flaps	Tail	Power
53(b) 53(c) 54(a) 54(b)	Standard and modified model	0 0 40 40 40	Closeddododododo	On -do- -do- On -do- Off	T _C = 0 0.4 normal rated power Normal rated power T _C = 0 0.4 normal rated power 0.4 normal rated power 0.4 normal rated power

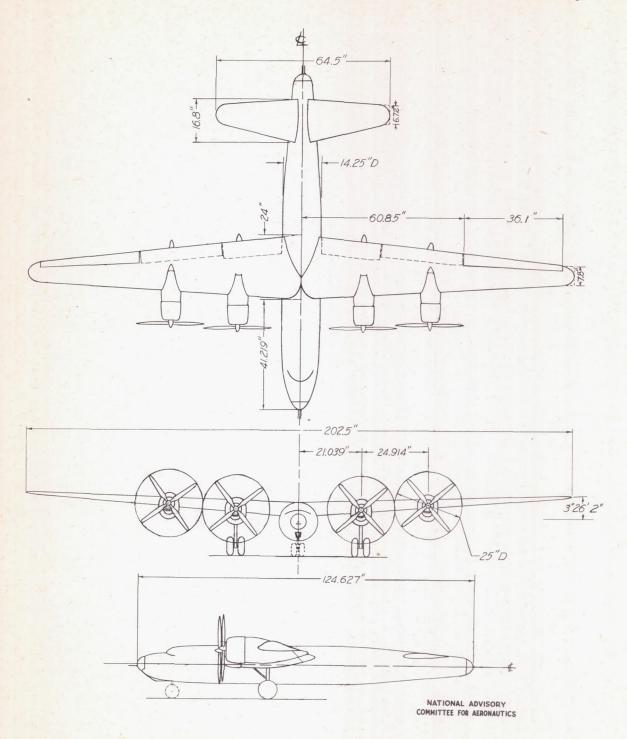
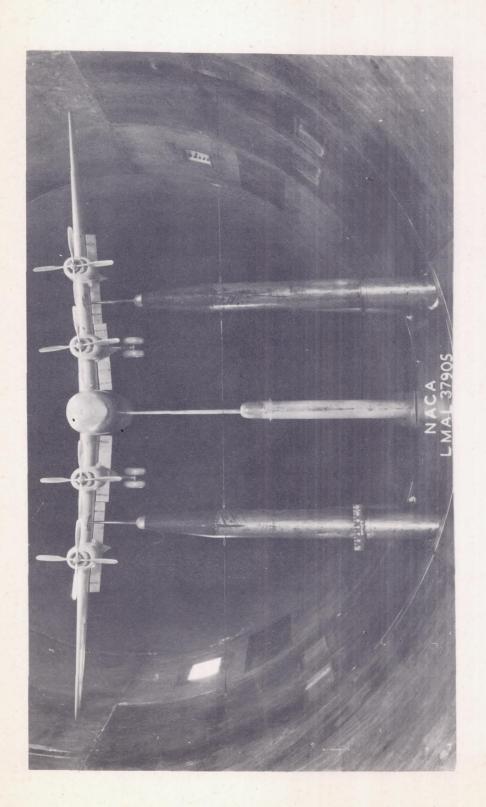


Figure 1. - Three-view drawing of model.



Model mounted in test section of Langley 19-foot pressure tunnel. 2.1 Figure

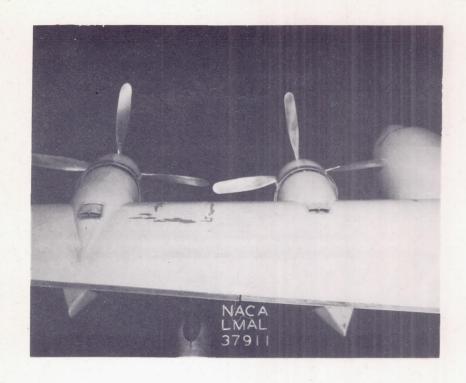




Figure 3.- Standard nacelles. $\delta_f = 0^{\circ}$.

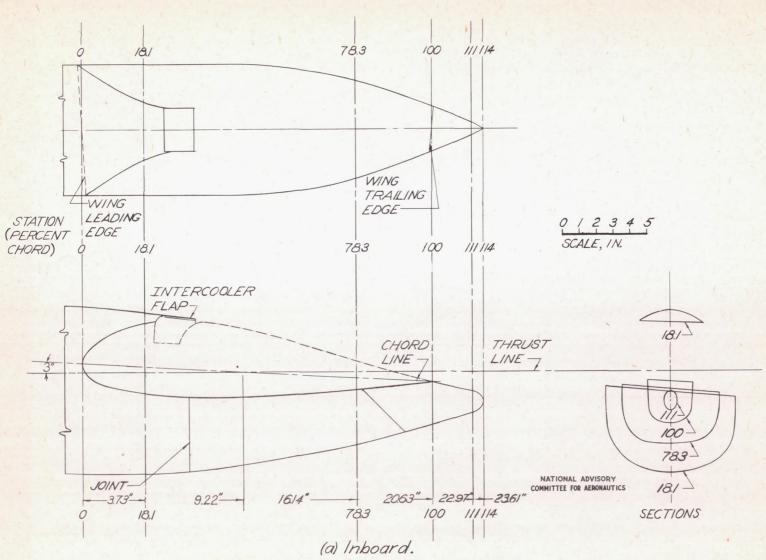
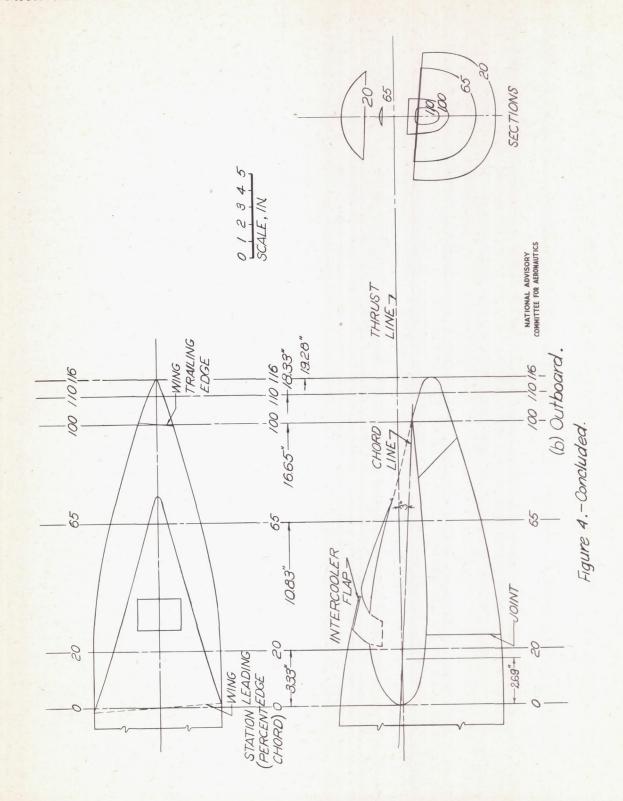
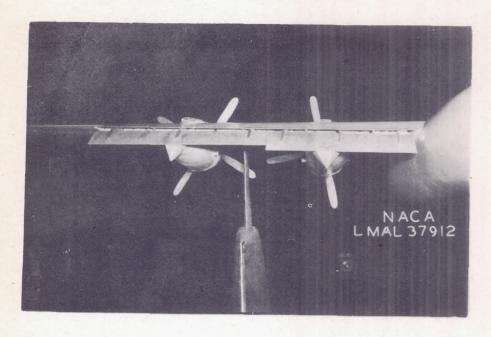


Figure 4.- Standard nacelle afterbody.





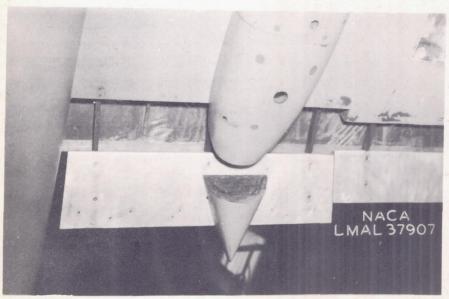
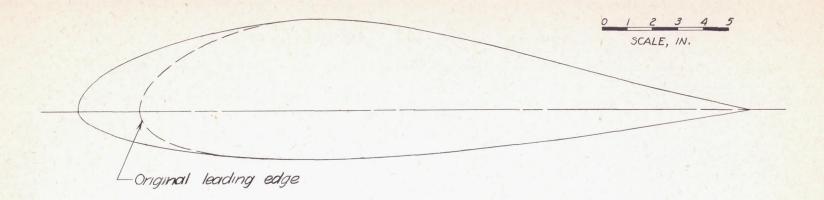


Figure 5.- Standard nacelles. $\delta_{\rm f}$ = 40°.



Ordinates of Wing Section with Leading-Edge Gloves at Model Center Line

Station ordinates in percent of wing chord

Station	Upper surface	Lower	Station	Upper surface	Lower
0 .5 .75 1.25 2.50 5.00 7.50 10 15 20 25 30 35	0 2.436 2.764 3.309 4.445 6.141 7.425 8.500 10.223 11.514 12.468 13.135 13.491	0 982 1.264 1.750 2.527 3.618 4.368 4.982 5.907 6.547 7.009 7.245 7.332	40 45 50 55 60 65 70 75 80 85 90 95	13.595 12.891 12.079 11.068 9.891 8.632 7.314 6.000 4.673 3.386 2.159 1.032	7.184 6.973 6.675 6.282 5.791 5.232 4.627 3.959 3.277 2.518 1.730 877

NATIONAL ADVISORY COMMITTEE FOR AERONAUTICS

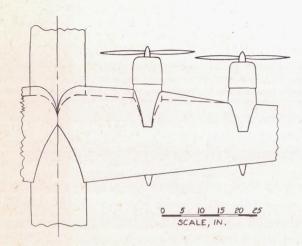
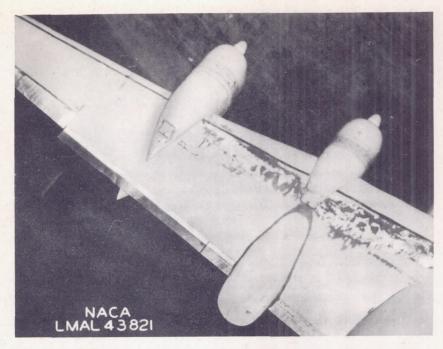


Figure 6 . - Details of leading-edge glove.



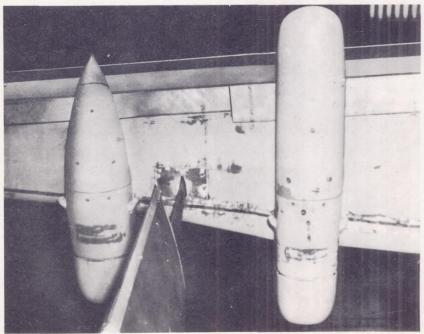


Figure 7.- Leading-edge gloves and trailing-edge extensions.



(a) Afterbody 2.



(b) Afterbody 3.

Figure 8. - Inboard nacelle afterbodies 2 and 3.

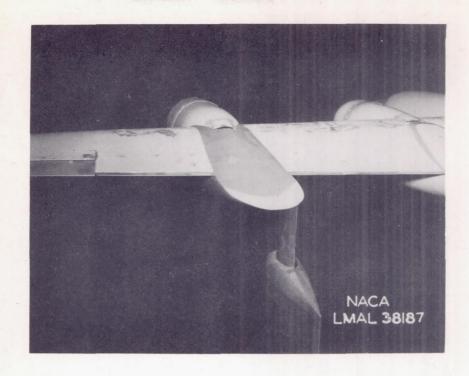




Figure 9.- Nacelle afterbody 4. $\delta_f = 0^{\circ}$.

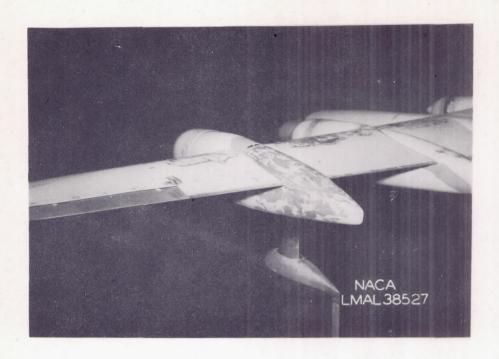
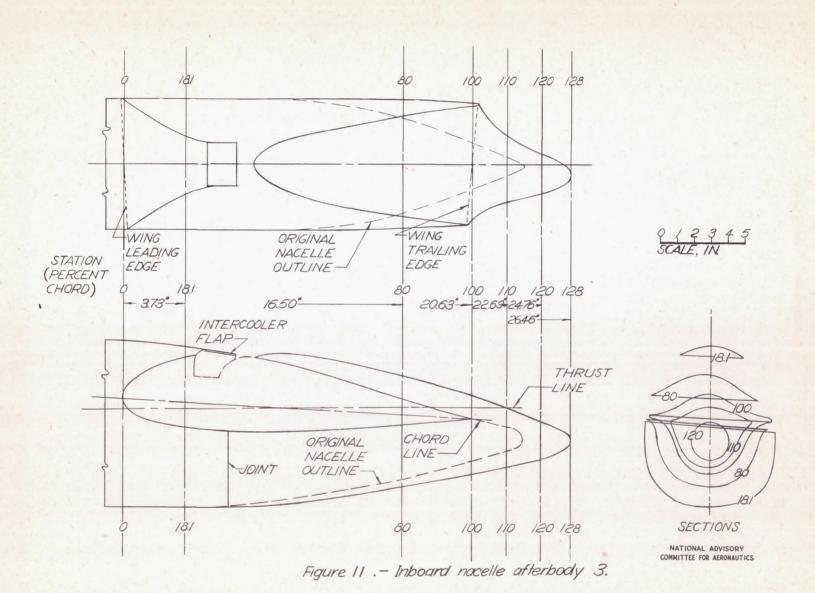
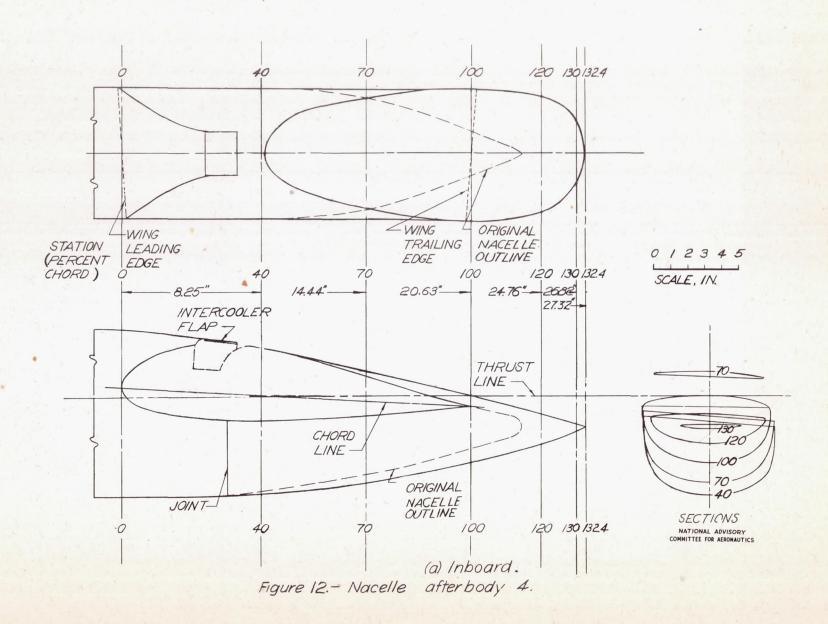
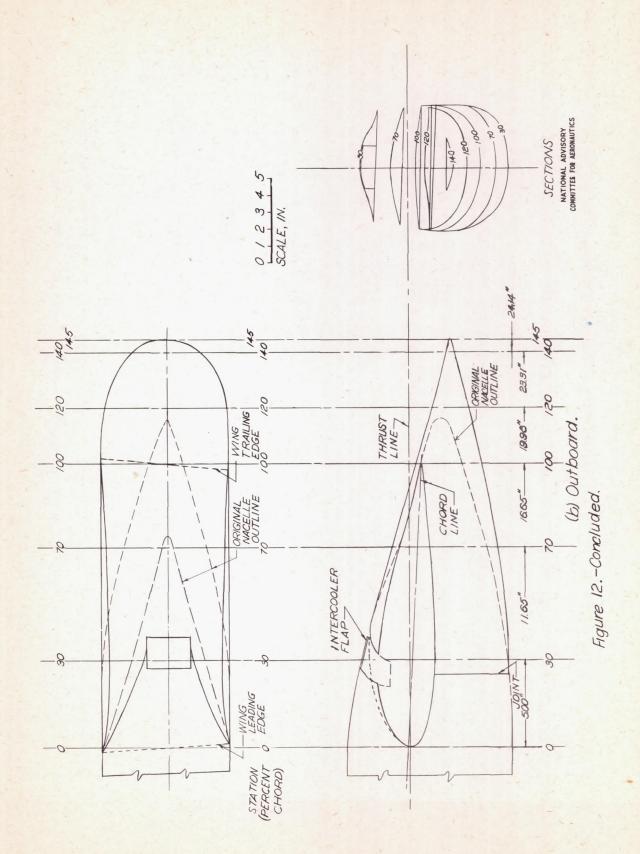




Figure 10.- Nacelle afterbody 5. $\delta_f = 0^{\circ}$.







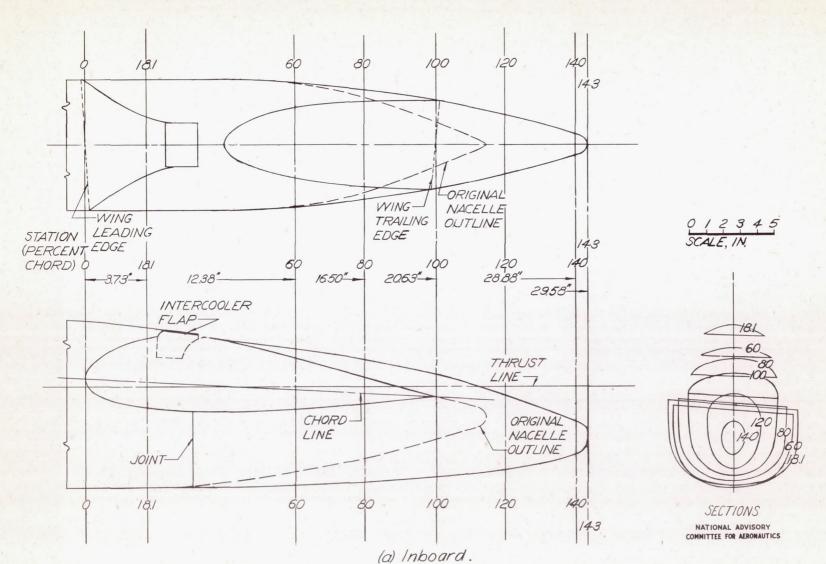


Figure 13. - Nacelle afterbody 5.

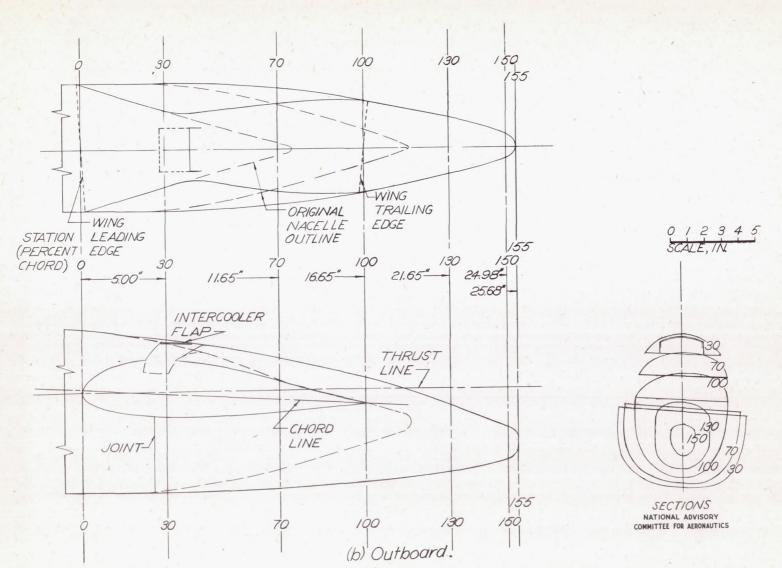


Figure 13.-Concluded.



Figure 14.- Inboard nacelle afterbody 4. $\delta_f = 40^{\circ}$.





Figure 15.- Inboard nacelle afterbody 5. $\delta_f = 40^{\circ}$.

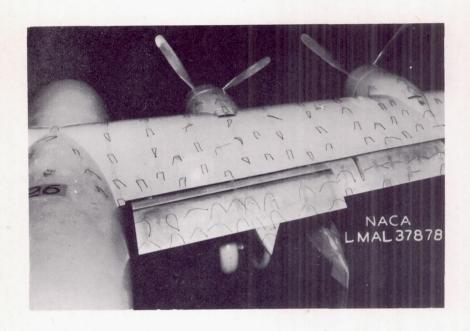




Figure 16. - Double slotted inboard flap.

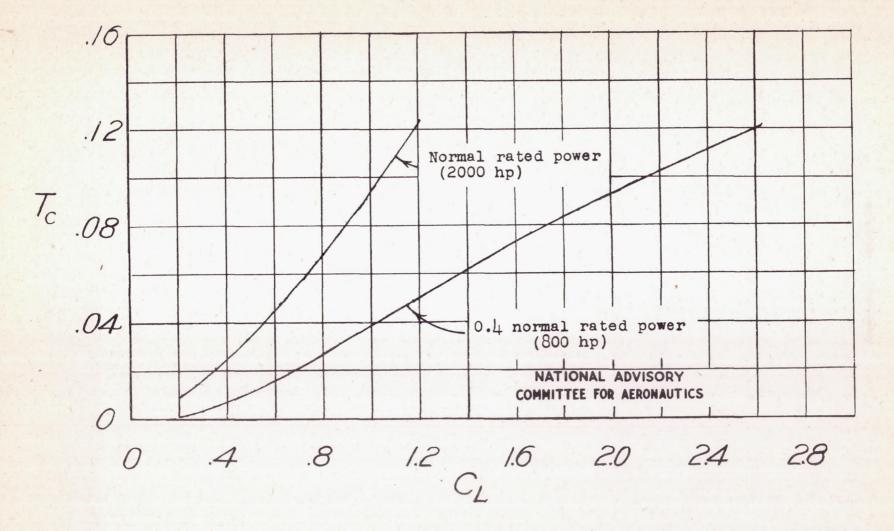


Figure 17. - Calculated thrust coefficient for one engine. Sea-level conditions.

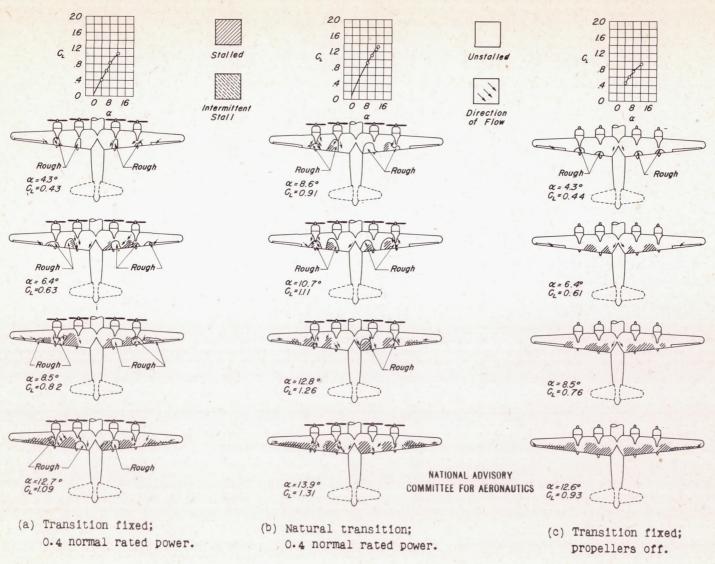


Figure 18.- Stall studies of model in standard configuration. $\delta_f = 0^\circ$; cowl and intercooler flaps closed; $R \approx 2,600,000$.

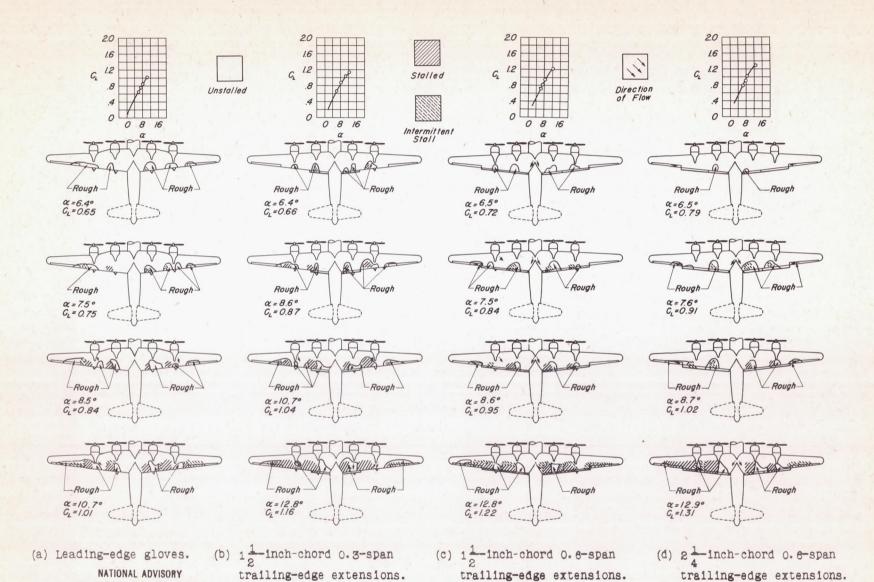
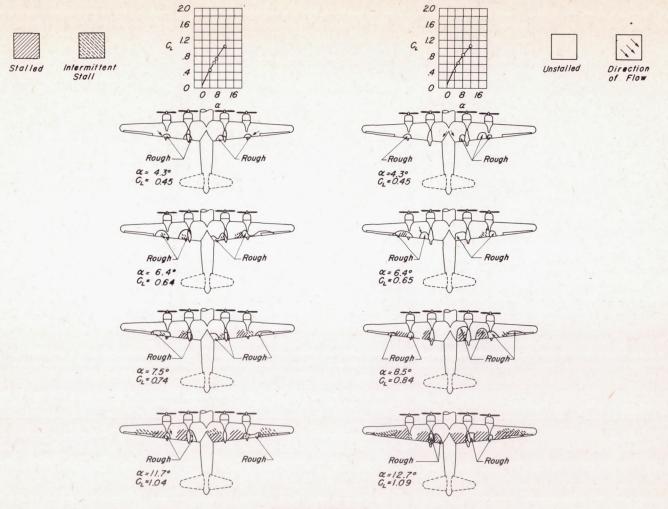


Figure 19.- Stall studies with leading-edge gloves and trailing-edge extensions. $\delta_{\rm f}=0^{\circ};$ cowl and intercooler flaps closed; 0.4 normal rated power; transition fixed; R $\approx 2,600,000.$

COMMITTEE FOR AERONAUTICS



(a) Afterbodies 2. COMMITTEE FOR AERONAUTICS (b) Afterbodies 3.

Figure 20.- Stall studies with modified inboard afterbodies 2 and 3. $\delta_f = 0^\circ$; cowland intercooler flaps closed; 0.4 normal rated power; transition fixed; $R \approx 2,600,000$.

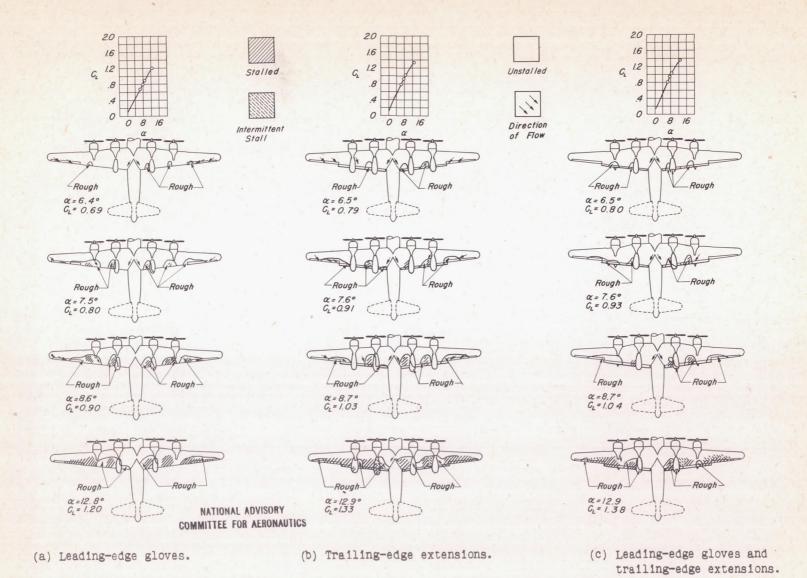


Figure 21.- Stall studies with afterbodies 4 and chord extensions. $\delta_f = 0^\circ$; cowland intercooler flaps closed; 0.4 normal rated power; transition fixed; $R \approx 2,600,000$.

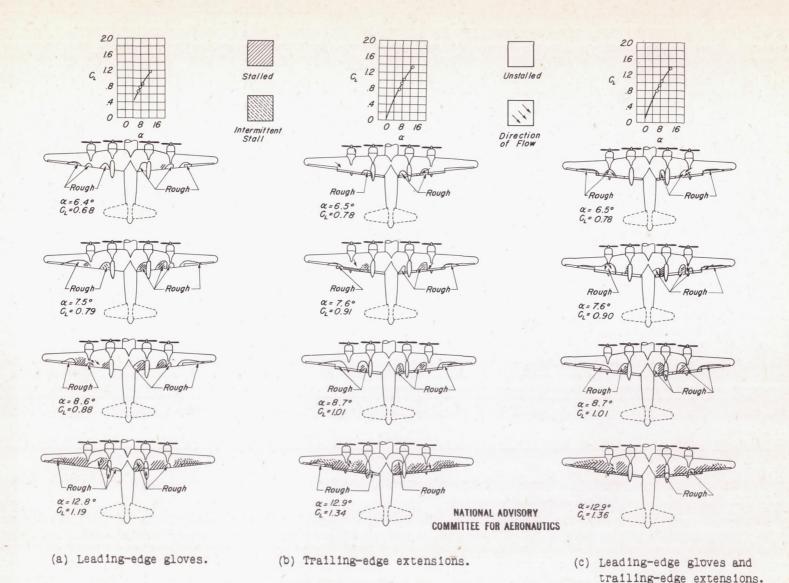


Figure 22.- Stall studies with afterbodies 5 and chord extensions. $\delta_f = 0^\circ$; cowl and intercooler flaps closed; 0.4 normal rated power; transition fixed; $R \approx 2,600,000$.

CL = 0.80 (

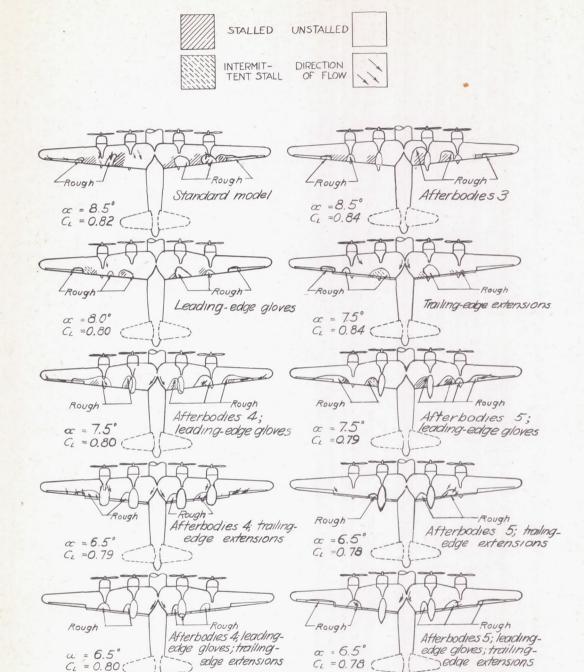
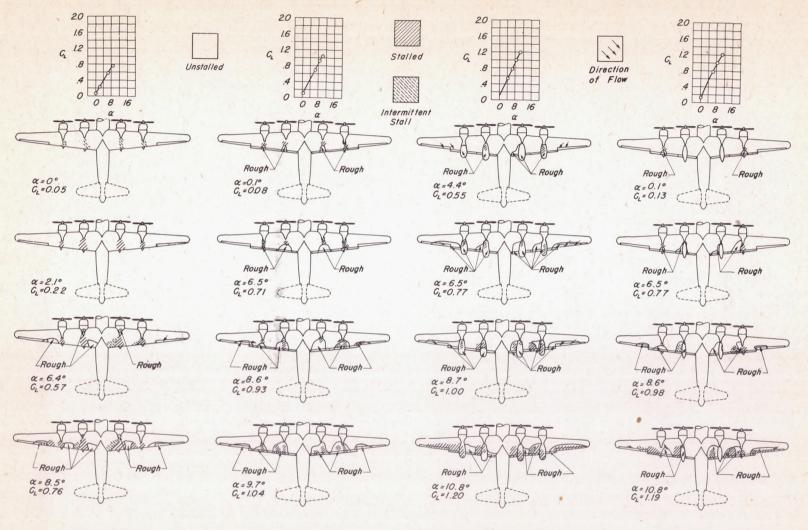


Figure 23. - Comparison of stall patterns with standard and modified model at a lift coefficient of approximately 0.8. of=0°; ccwl and intercooler flaps closed; 0.4 normal rated power; transition fixed; $R \approx 2,600,000$.

CL = 0.78

NATIONAL ADVISORY COMMITTEE FOR AERONAUTICS



- (a) Standard model.
- (b) Trailing-edge extensions.
- (c) Afterbodies 4 and trailing-edge extensions.
- (d) Inboard afterbodies 5 and trailing-edge extensions.

NATIONAL ADVISORY
COMMITTEE FOR AERONAUTICS

Figure 24.- Stall studies of standard and modified models. $\delta_f = 0^\circ$; cowl and intercooler flaps open; 0.4 normal rated power; transition fixed; $R \approx 2,600,000$.

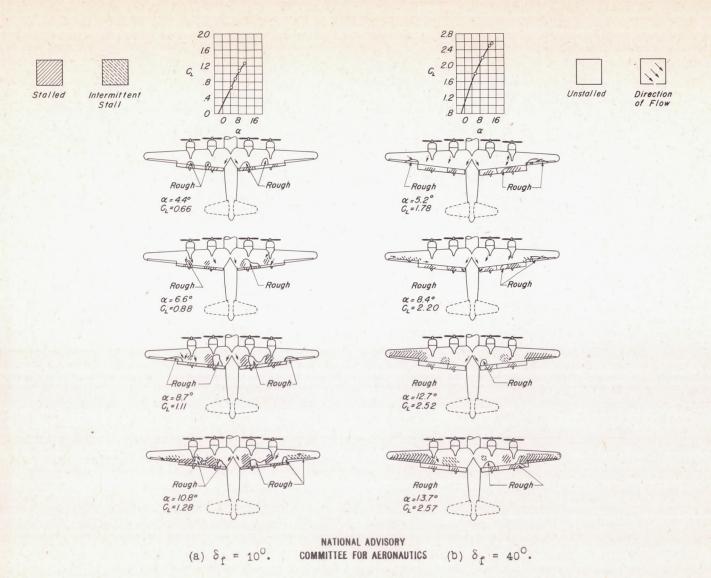


Figure 25. - Stall studies of standard model with wing flaps deflected. Cowl and intercooler flaps closed; 0.4 normal rated power; transition fixed; $R \approx 2,600,000$.

edge extensions cut out;

 $a = 11.8^{\circ}$.

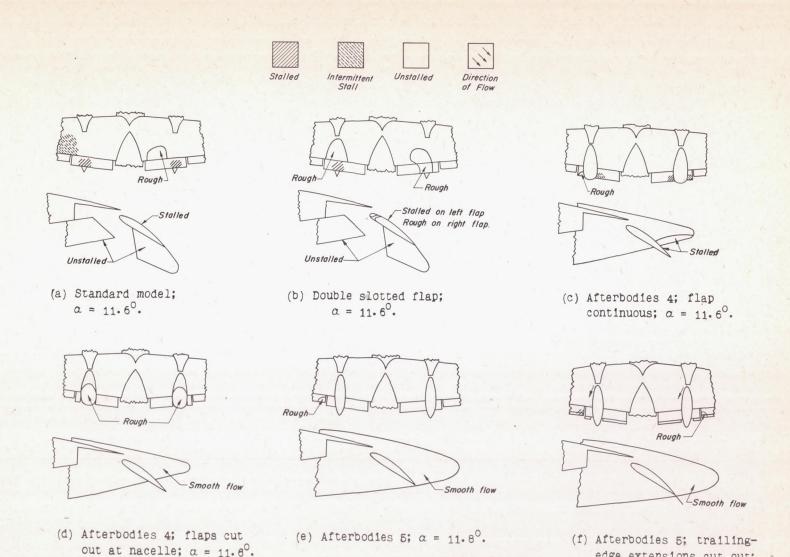
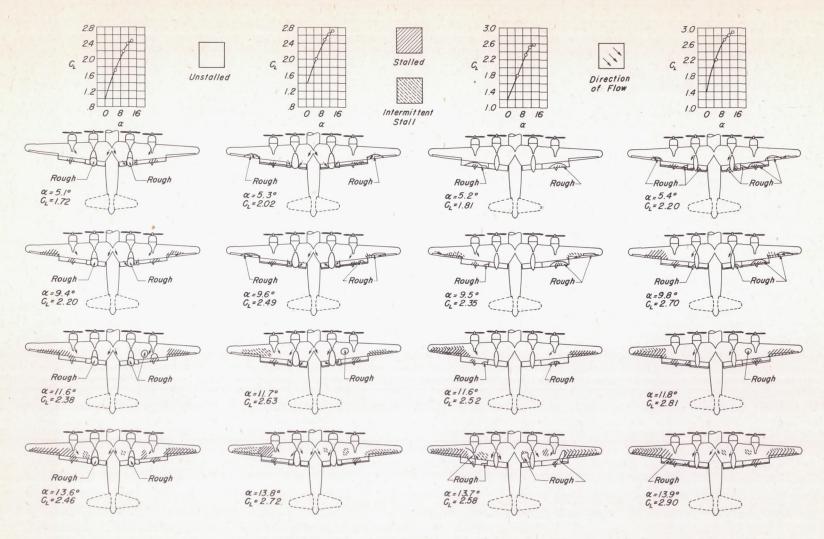


Figure 26.- Flow over inboard flaps and afterbodies. $\delta_f = 40^\circ$; cowl and intercooler flaps closed; 0.4 normal rated power; transition fixed; $R \approx 2,600,000$.

NATIONAL ADVISORY

COMMITTEE FOR AERONAUTICS



(a) Afterbodies 4; flaps cut out. (b) Afterbodies 4; flaps and trailing-edge extensions cut out.

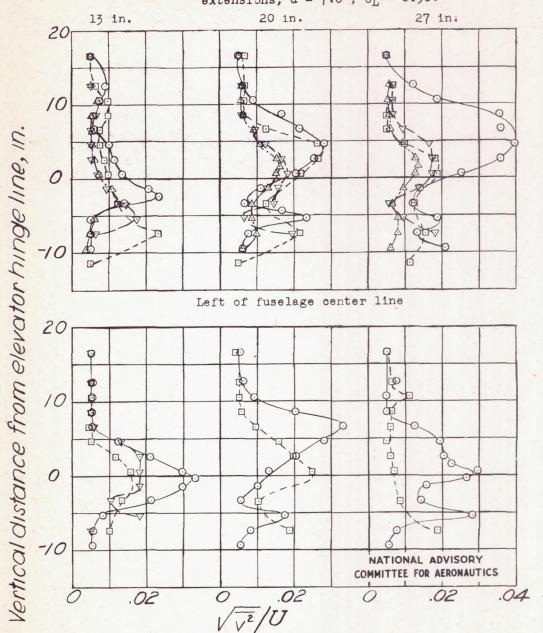
(c) Afterbodies 5.

(d) Afterbodies 5; trailing-edge extensions cut out.

NATIONAL ADVISORY COMMITTEE FOR AERONAUTICS

Figure 27.- Stall studies of modified model. $\delta_f = 40^\circ$; cowl and intercooler flaps closed; 0.4 normal rated power; transition fixed; R≈ 2,600,000.

O Standard configuration; $a = 7.5^{\circ}$; $c_L = 0.73^{\circ}$ A Inboard afterbodies 4 and trailing-edge extensions; $a = 7.6^{\circ}$; $c_L = 0.91^{\circ}$ Inboard afterbodies 5 and trailing-edge extensions; $a = 7.6^{\circ}$; $c_L = 0.91^{\circ}$ V Leading-edge gloves, inboard afterbodies 5, and trailing-edge extensions; $a = 7.6^{\circ}$; $c_L = 0.90^{\circ}$.



Right of fuselage center line

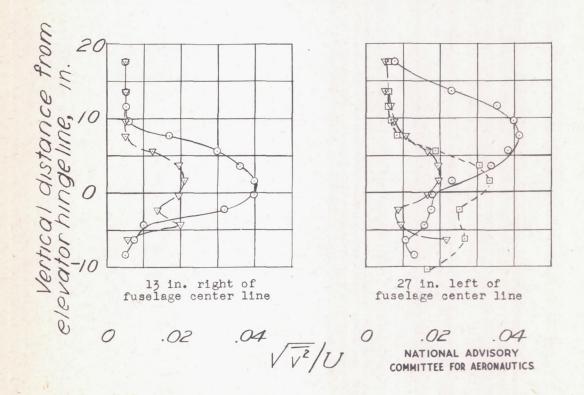
(a) $\alpha \approx 7.6^{\circ}$.

Figure 28.- Vertical velocity deviations in region of horizontal tail for standard and modified models. $\delta_f = 0^\circ$; cowl and intercooler flaps closed; transition fixed; 0.4 normal rated power; $R \approx 2,600,000$.

O Standard configuration; a = 8.5; C_L = 0.82

Inboard afterbodies 5 and trailing-edge extensions; a=8.7; C_L=1.01

V Leading-edge gloves, inboard afterbodies 5, and trailing-edge extensions; a = 8.7; C_L = 1.01



(b) $\alpha \approx 8.7^{\circ}$.

Figure 28. - Concluded.

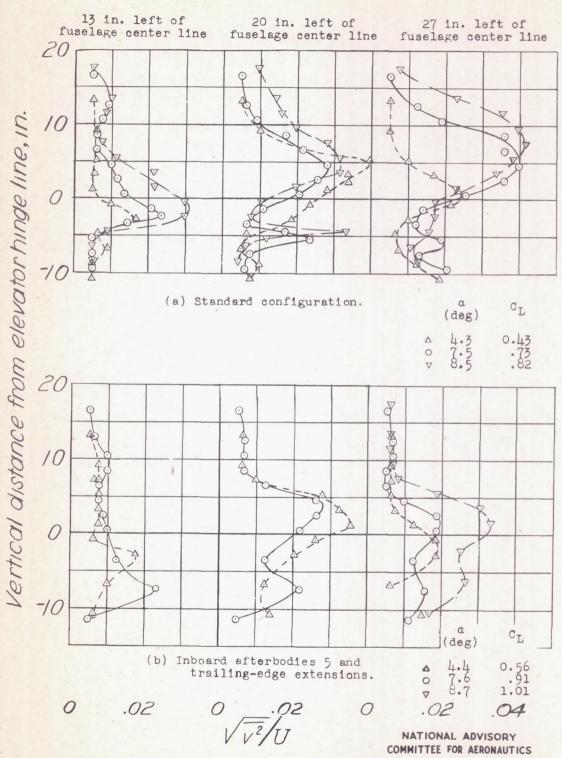


Figure 29.- Effect of angle of attack on vertical velocity deviations in region of horizontal tail for standard and modified models. $\delta_f = 0^\circ$; cowl and intercooler flaps closed; transition fixed; 0.4 normal rated power; $R \approx 2,600,000$.

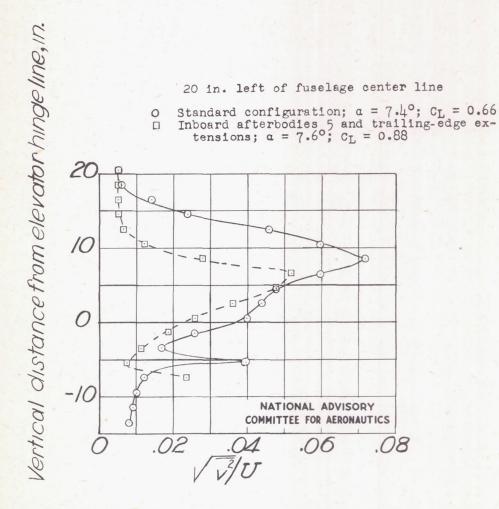


Figure 30.- Vertical velocity deviations in region of horizontal tail for standard and modified models. $\delta_f = 0^\circ$; cowl and intercooler flaps open; transition fixed; 0.4 normal rated power; $R \approx 2,600,000$.

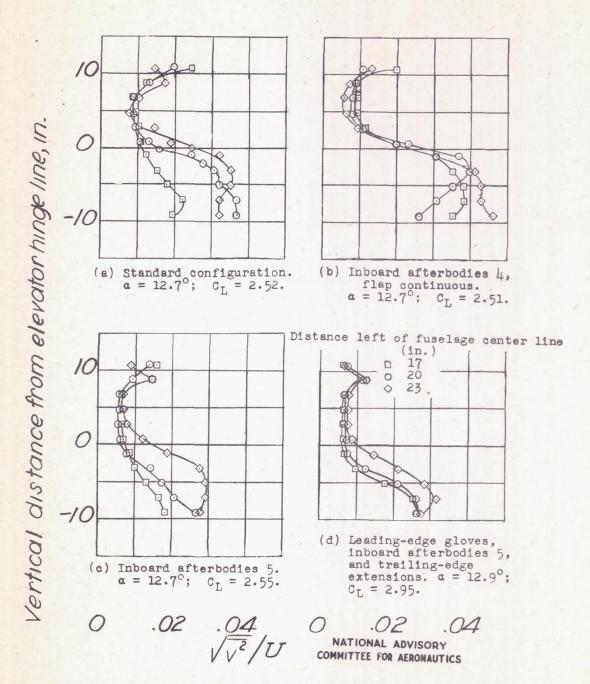


Figure 31.- Vertical velocity deviations in region of horizontal tail for standard and modified models. $\delta_f=40^\circ$; cowl and intercooler flaps closed; transition fixed; 0.4 normal rated power; R \approx 2,600,000.

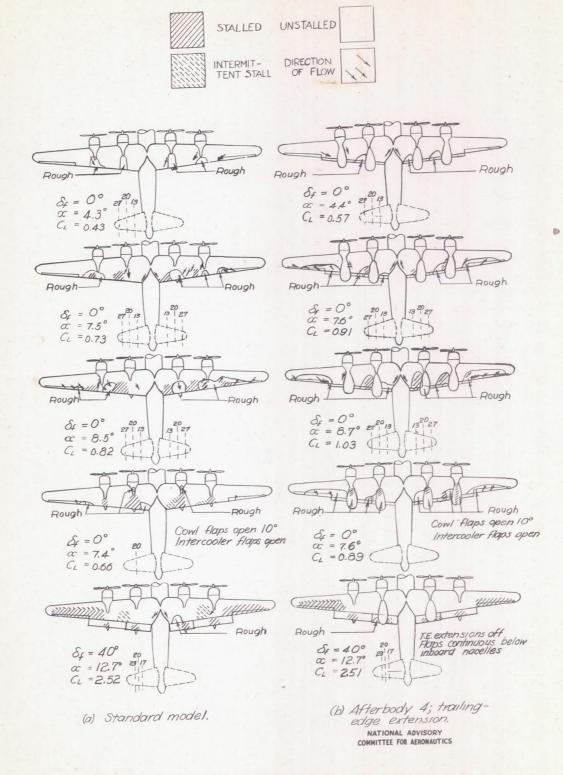


Figure 32.- Stall patterns for conditions of turbulence surveys. Transition fixed; 0.4 normal rated power; $R \approx 2,600,000$.

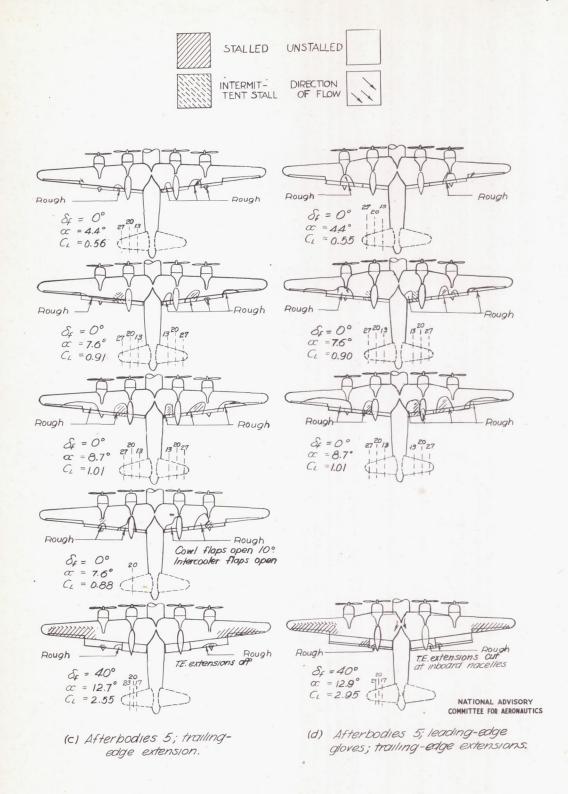


Figure 32 .- Concluded.

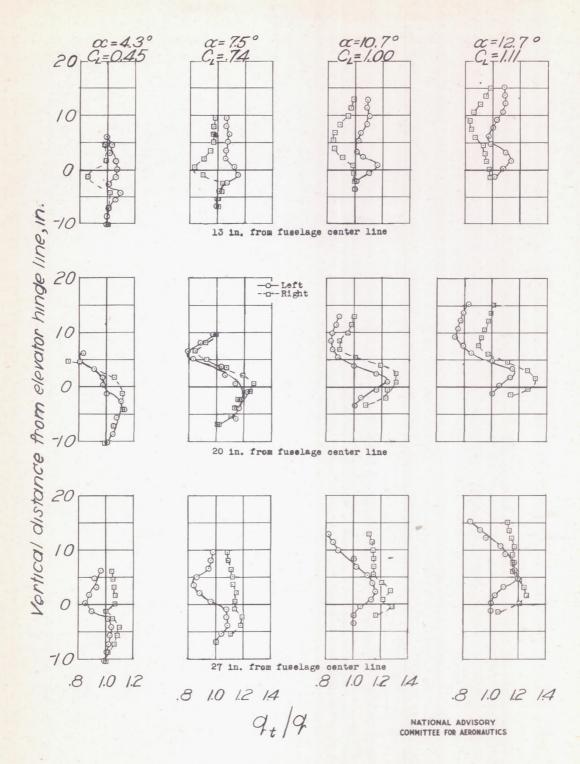


Figure 33.- Dynamic-pressure variation in the region of the horizontal tail. Standard configuration; $\delta_f = 0^\circ$; cowl and intercooler flaps closed; transition fixed; 0.4 normal rated power; R $\approx 2,600,000$.

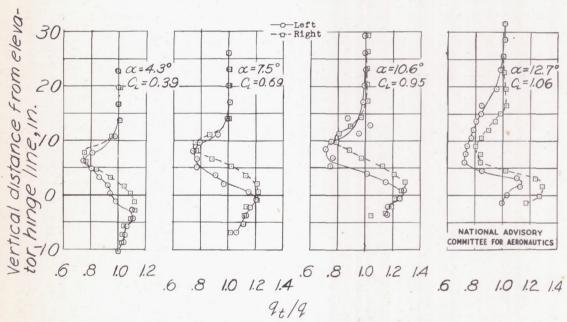


Figure 34.- Dynamic-pressure variation in the region of the horizontal tail, 20 inches from fuselage center line. Stendard configuration; $\delta_{\rm f}=0^{\circ};$ cowl and intercooler flaps open; transition fixed; 0.4 normal rated power; R \approx 2,600,000.

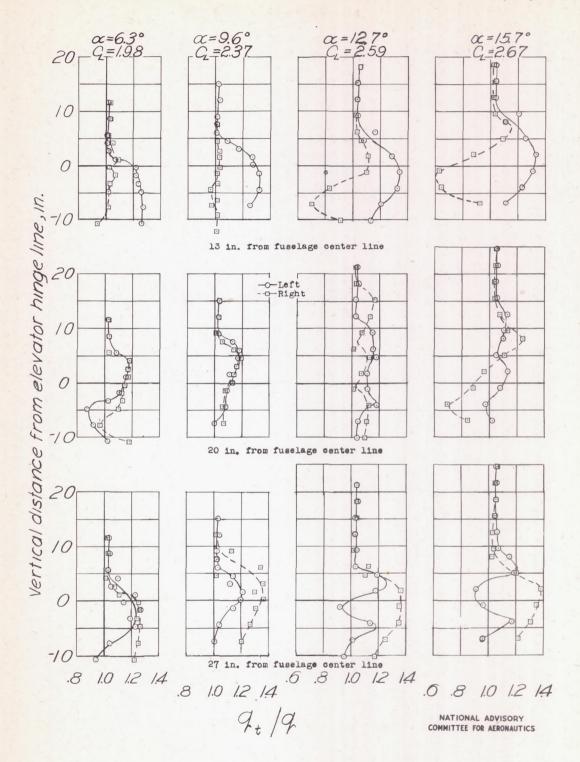
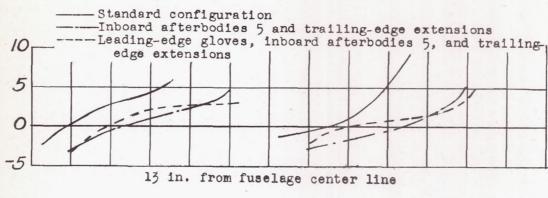


Figure 35.- Dynamic-pressure variation in the region of the horizontal tail. Standard configuration; $\delta_{\bf f} = 40^{\circ}$; cowl and intercooler flaps closed; transition fixed; 0.4 normal rated power; R \approx 2,600,000.



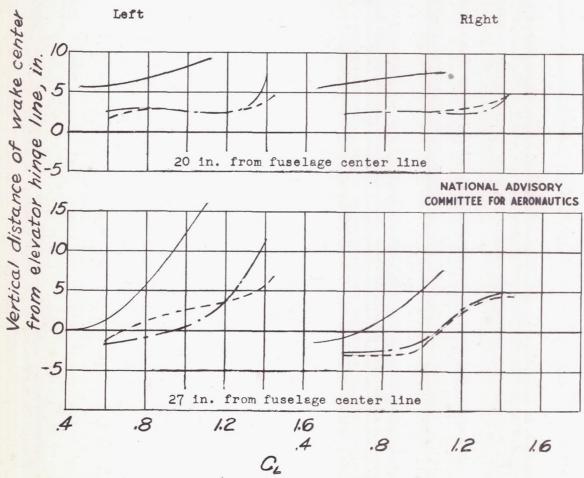


Figure 36.- Variation of location of dynamic-pressure wake center with lift coefficient. $\delta_f = 0^\circ$; cowl and intercooler flaps closed; transition fixed; 0.4 normal rated power; $R \approx 2,600,000$.

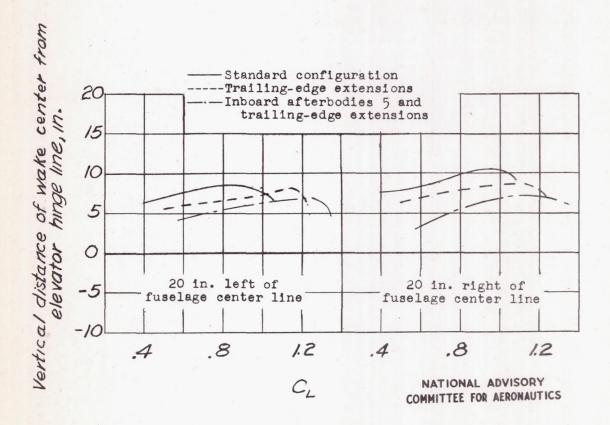


Figure 37.- Variation of location of dynamic-pressure wake center with lift coefficient. $\delta_f = 0^\circ$; cowl and intercooler flaps open; transition fixed; 0.4 normal rated power; R \approx 2,600,000.



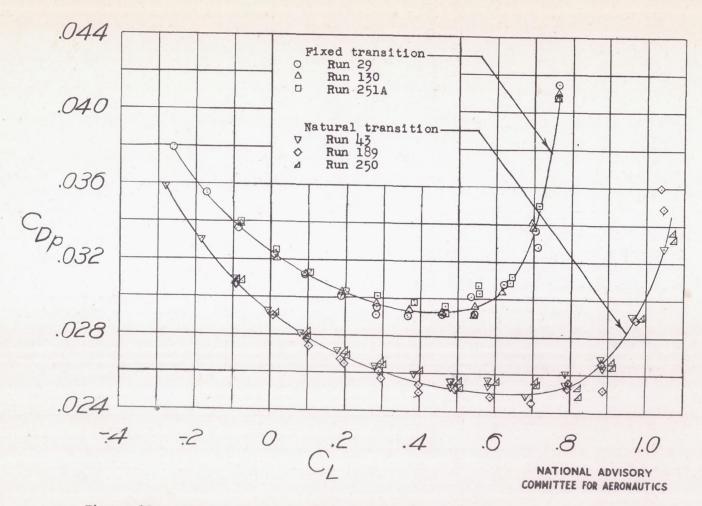
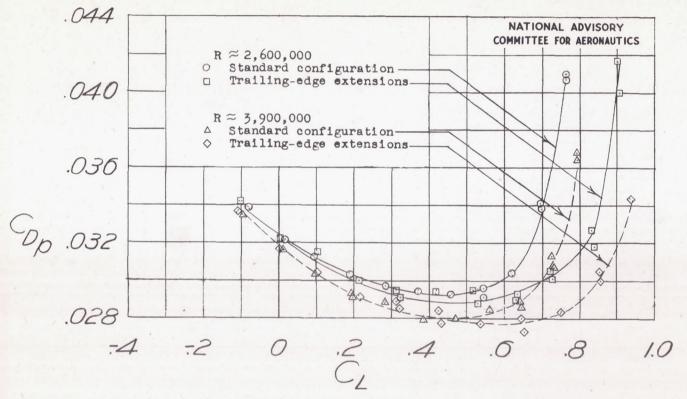
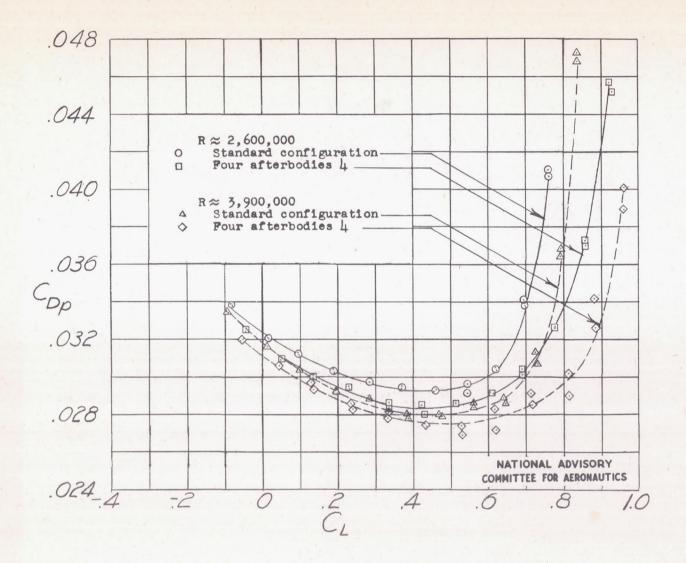


Figure 38 .- Drag characteristics obtained from several runs with model in the standard configuration. $\delta_f = 0^\circ$; cowl and intercooler flaps closed; $R \approx 2,600,000$.

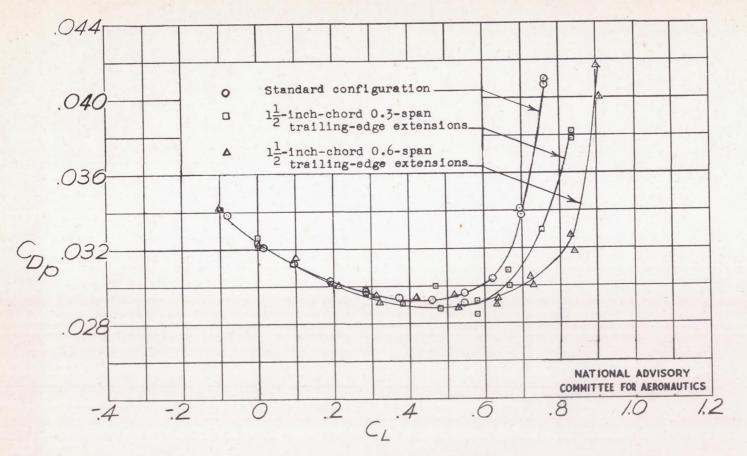


(a) Trailing-edge extensions having $1\frac{1}{2}$ -inch chord and 0.6 span.

Figure 39.- Drag characteristics at two Reynolds numbers for standard and modified models. δ_f = 0°; cowl and intercooler flaps closed; fixed transition.

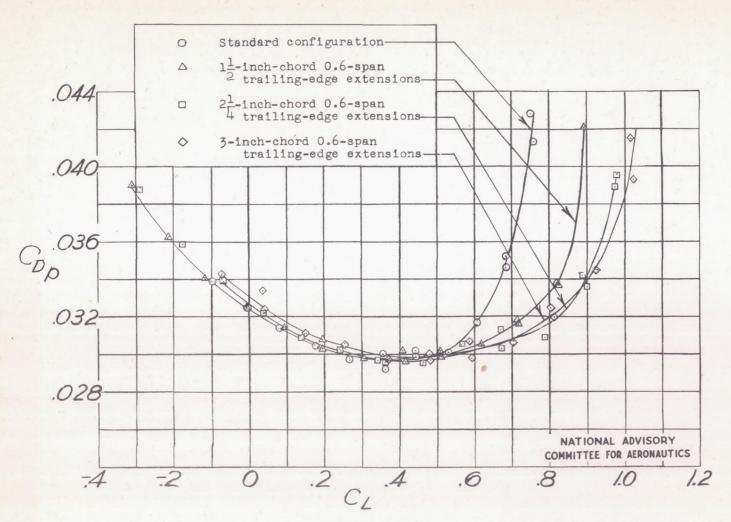


(b) Modified afterbodies.Figure 39 .- Concluded.



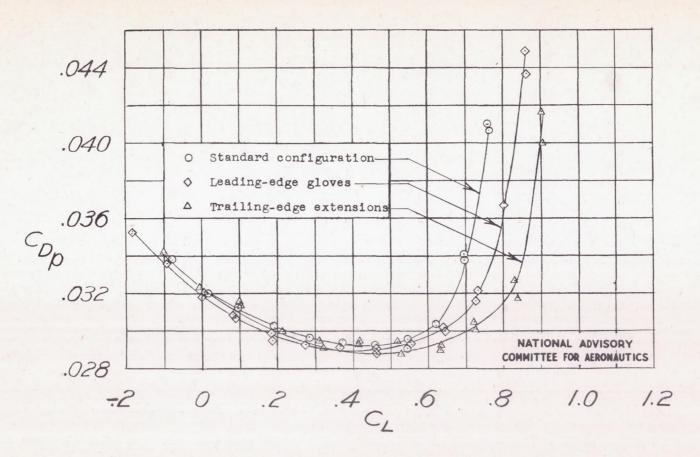
(a) Effect of span.

Figure 40.- Drag characteristics with several trailing-edge extensions. $\delta_f = 0^\circ$; cowl and intercooler flaps closed; fixed transition; $R \approx 2,600,000$.



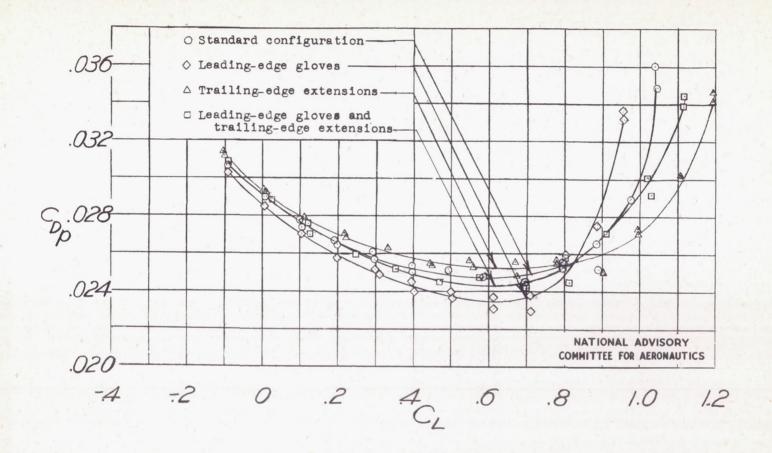
(b) Effect of chord.

Figure 40 .- Concluded.



(a) Fixed transition.

Figure 41 .- Drag characteristics with leading-edge gloves and trailing-edge extensions. $\delta_f = 0^\circ$; cowl and intercooler flaps closed; $R \approx 2,600,000$.



(b) Natural transition.

Figure 41 .- Concluded.

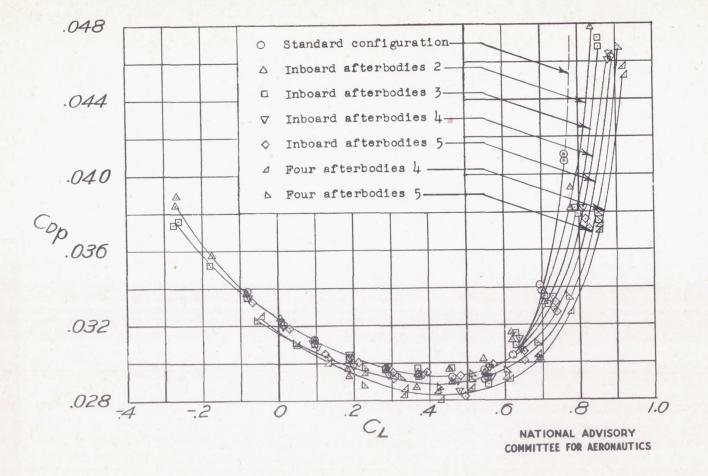
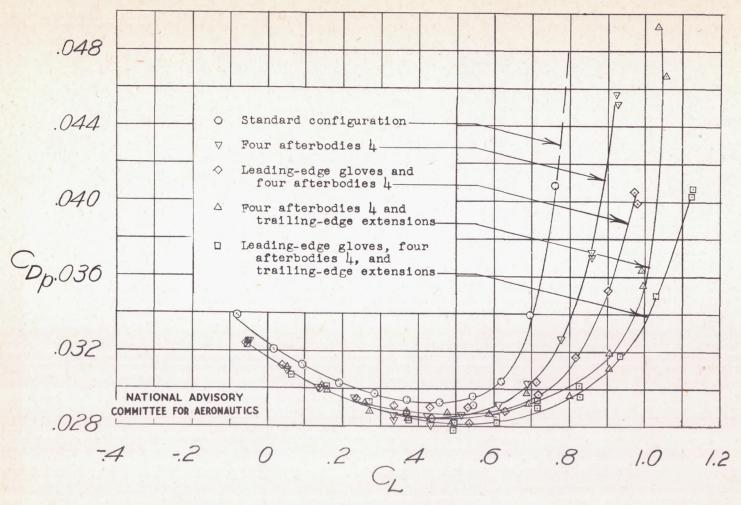
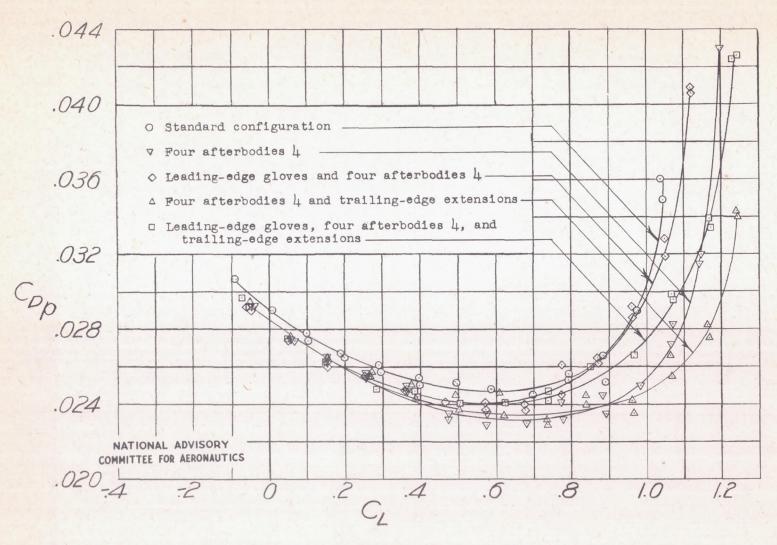


Figure 42.- Drag characteristics with modified afterbodies. $\delta_f = 0^\circ$; cowl and intercooler flaps closed; fixed transition; $R \approx 2,600,000$.



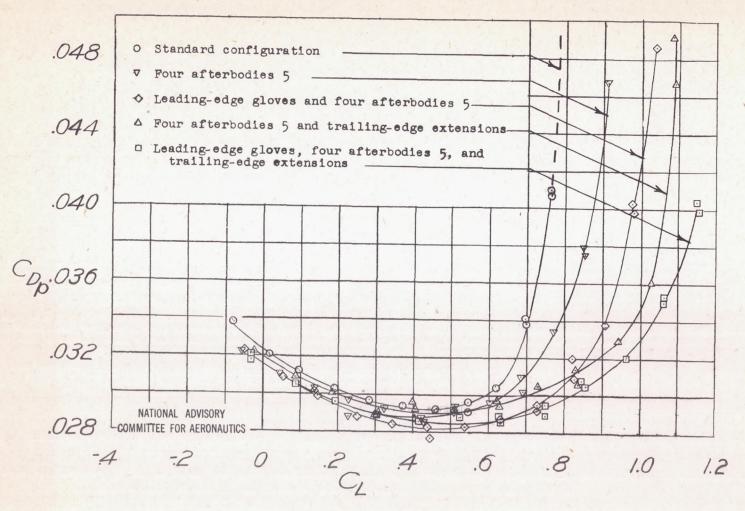
(a) Fixed transition.

Figure 43.- Drag characteristics with afterbodies 4 alone and with chord extensions. $\delta_{\rm f}=0^{\circ};$ cowl and intercooler flaps closed; R \approx 2,600,000.



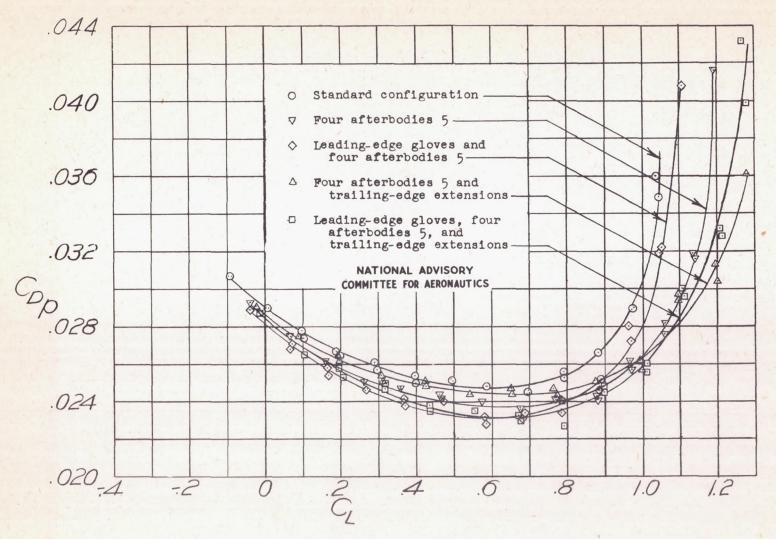
(b) Natural transition.

Figure 43. - Concluded.



(a) Fixed transition.

Figure 44.- Drag characteristics with afterbodies 5 alone and with chord extensions. $\delta_f=0^\circ;$ cowl and intercooler flaps closed; R \approx 2,600,000.



(b) Natural transition.

Figure 44. - Concluded.

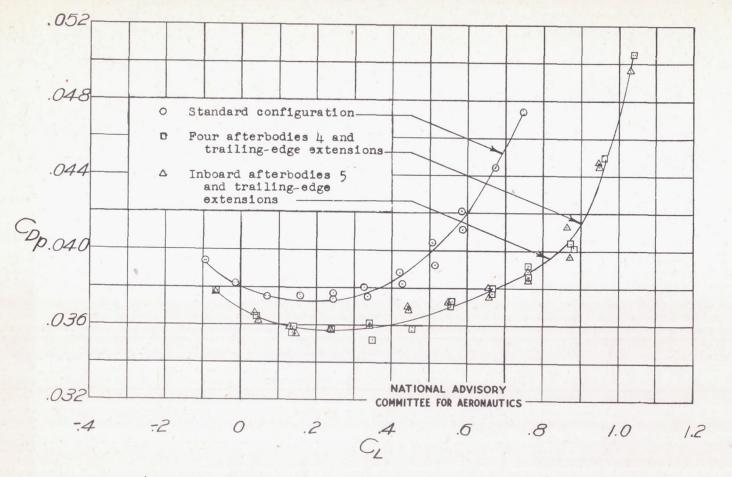


Figure 45.- Drag characteristics with cowl and intercooler flaps open for standard and modified models. $\delta_f=0$; fixed transition; R \approx 2,600,000.

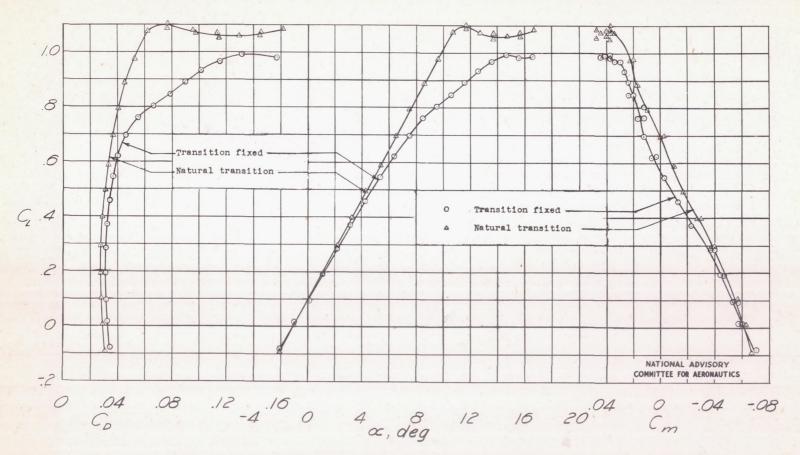


Figure 46.- Aerodynamic characteristics with fixed and natural transition. Standard configuration; $\delta_f = 0^\circ$; cewl and intercooler flaps closed; $R \approx 2,600,000$; propellers eff.

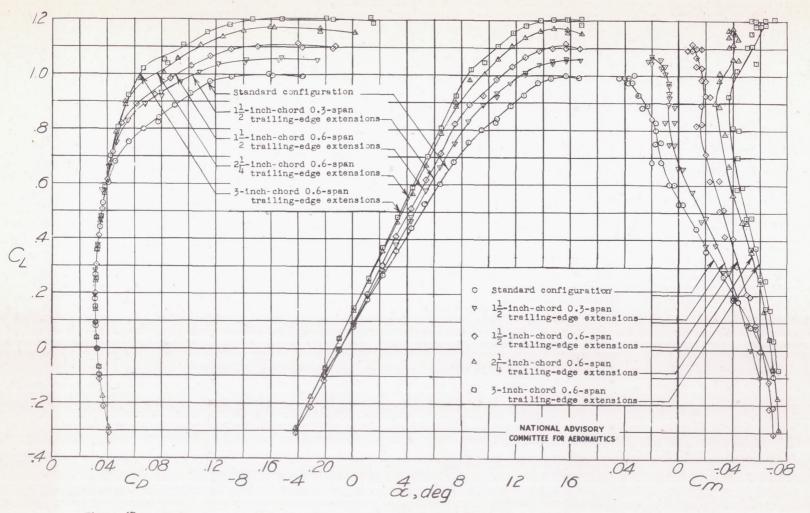
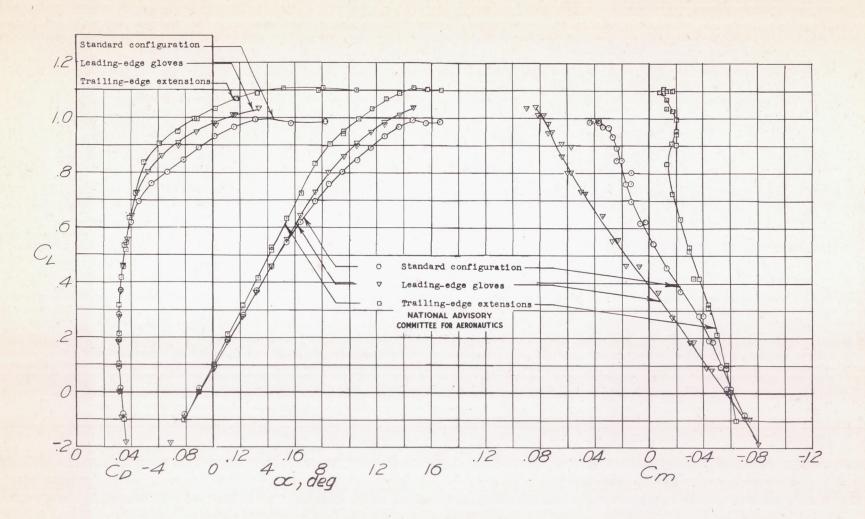


Figure 47.- Aerodynamic characteristics with several trailing-edge extensions. $\delta_{\mathbf{f}}=0^{\circ}$; cowl and intercooler flaps closed; fixed transition; $R\approx2,600,000$; propellers off.



(a) Fixed transition.

Figure 48 .- Aerodynamic characteristics with leading-edge gloves and trailing-edge extensions. $\delta_{\bf f}=0^{\circ};$ cowl and intercooler flaps closed; ${\rm R}\approx 2,600,000;$ propellers off.

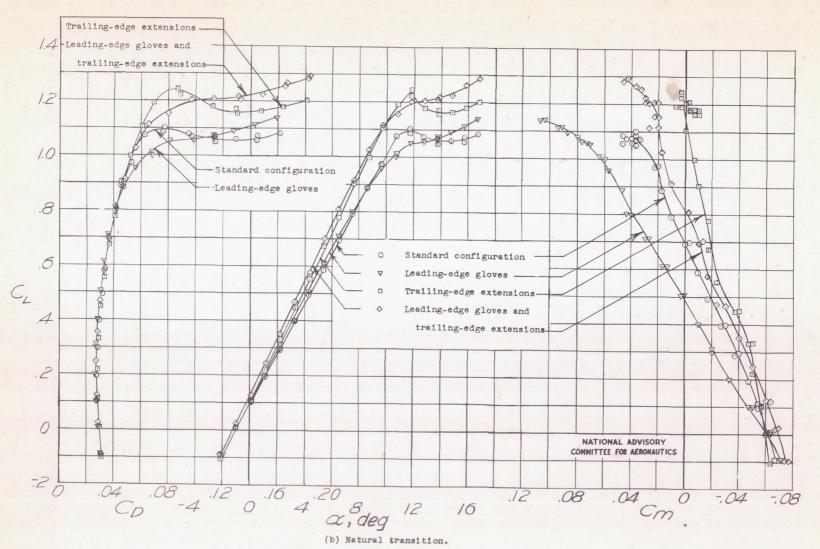


Figure 48 .- Concluded.

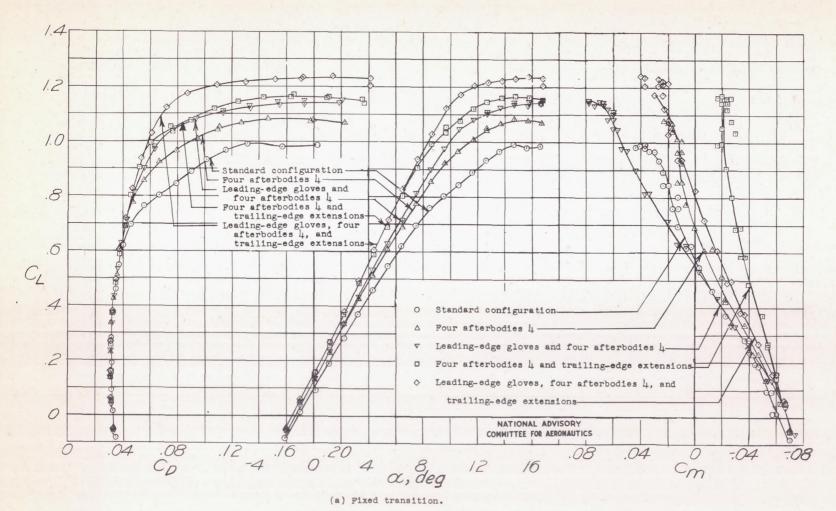
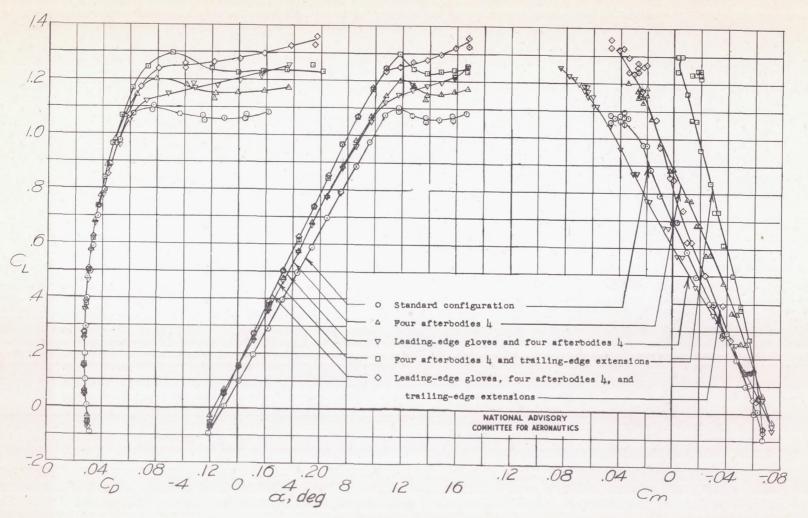


Figure 49.- Aerodynamic characteristics with afterbodies 4 alone and with chord extensions. $\delta_{\mathbf{f}} = 0^{\circ}$; cowl and intercooler flaps closed; $R \approx 2,600,000$; propellers off.



(b) Natural transition.
Figure 49.- Concluded.

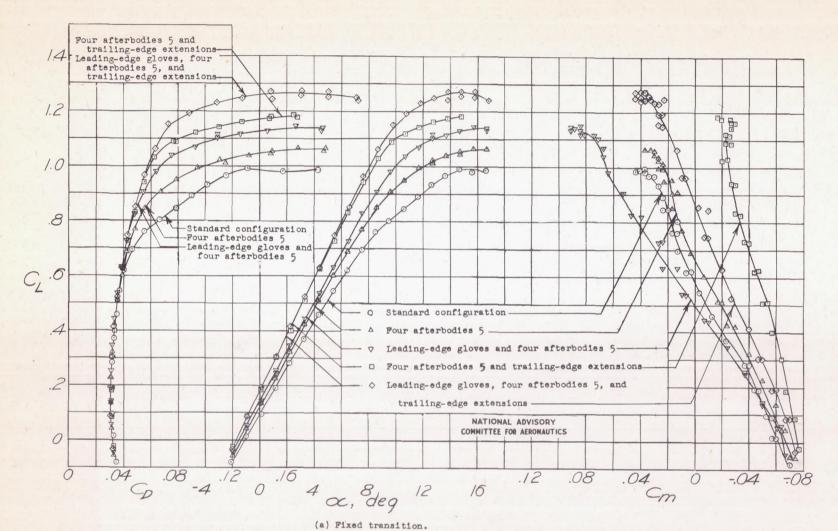
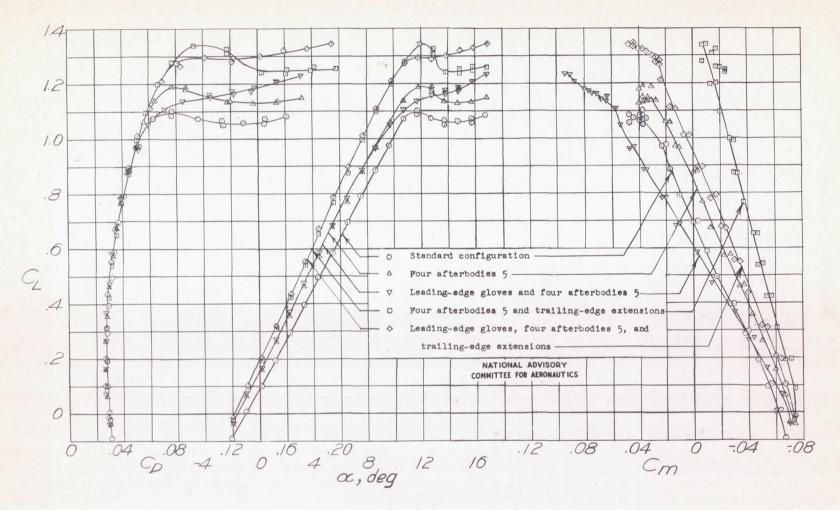


Figure 50.- Aerodynamic characteristics with afterbodies 5 alone and with chord extensions. $\delta_f = 0^\circ$; cowl and intercooler flaps closed; $R \approx 2,600,000$; propellers off.



(b) Natural transition.

Figure 50 .- Concluded.

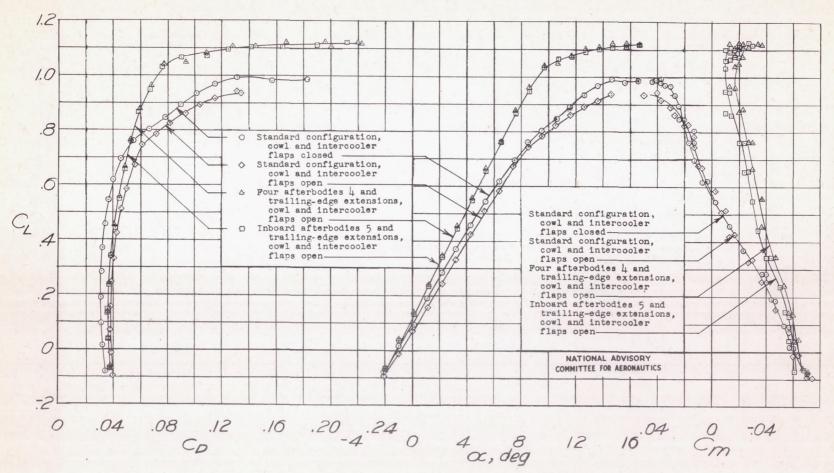


Figure 51.- Aerodynamic characteristics with cowl and intercooler flaps open for standard and modified models. $\delta_f = 0^0; \text{ fixed transition; } R \approx 2,600,000; \text{ propellers off.}$

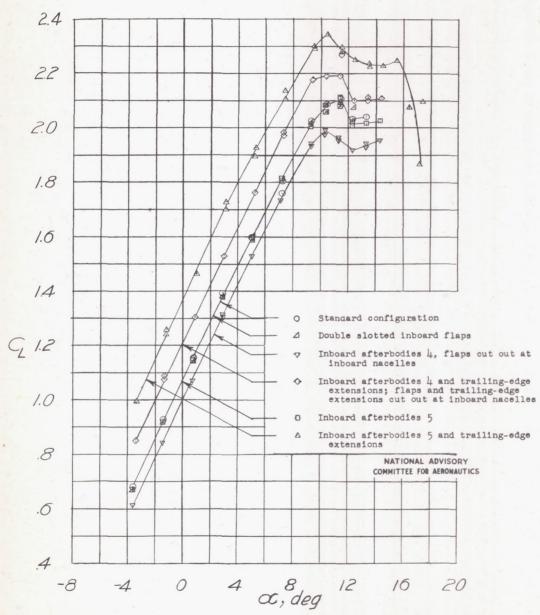
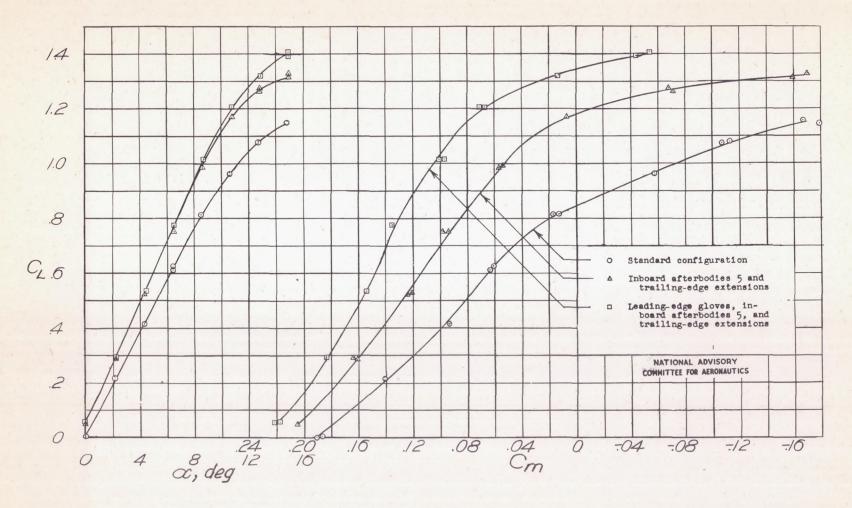
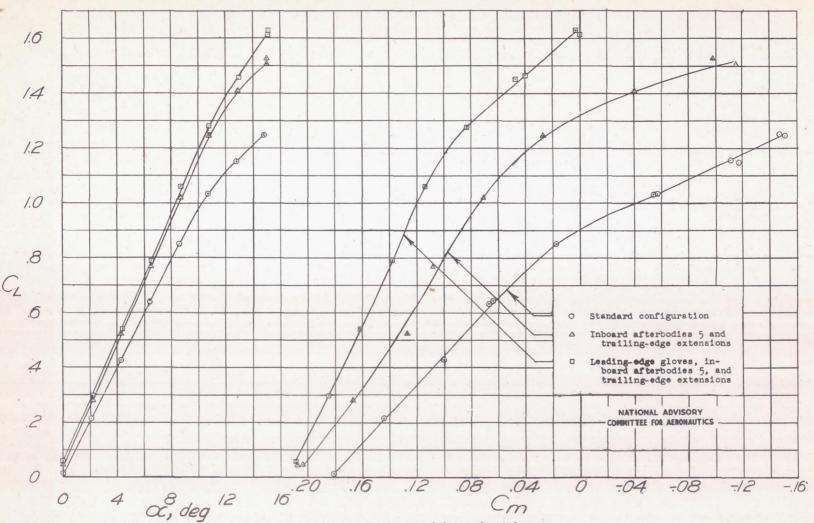


Figure 52.- Lift characteristics with wing flaps deflected for standard and modified models. $\delta_f = 40^\circ$; cowl and intercooler flaps closed; fixed transition; $R \approx 2,600,000$; propellers off.



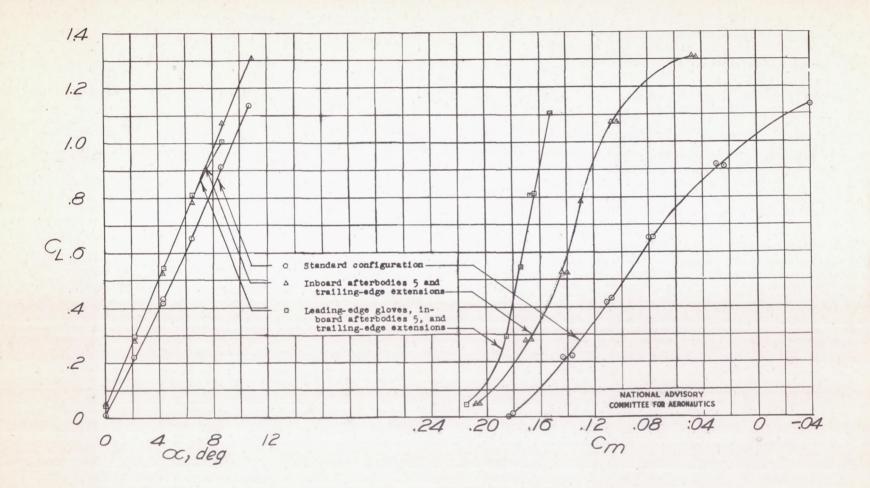
(a) $T_{c} = 0$.

Figure 53.- Effect of modifications on pitching moment and lift. $\delta_f = 0^\circ$; cowl and intercooler flaps closed; horizontal tail on; transition fixed; $R \approx 2,600,000$.

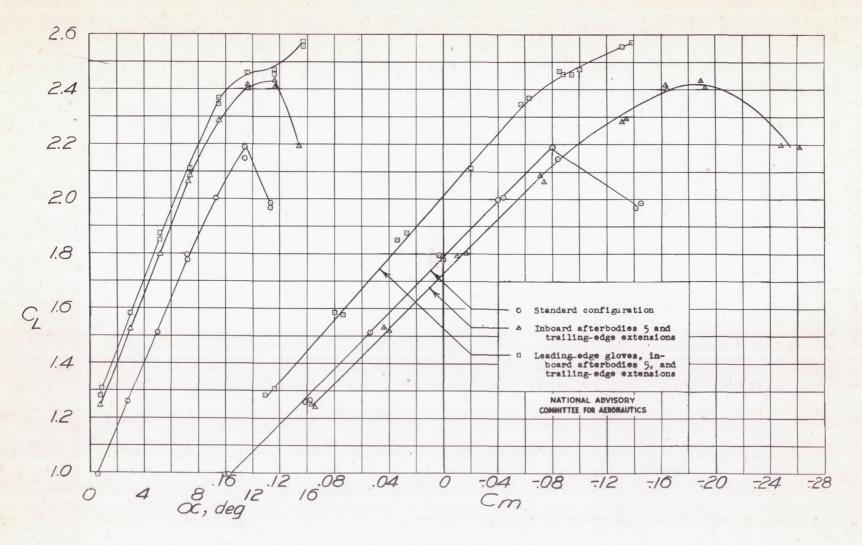


(b) Propellers operating at 0.4 normal rated power.

Figure 53. - Continued.

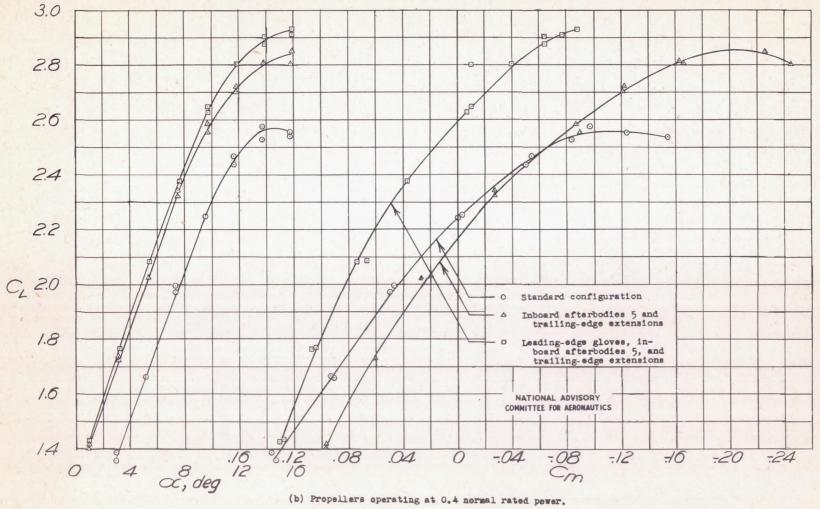


(c) Normal rated power.
Figure 55 .- Concluded.

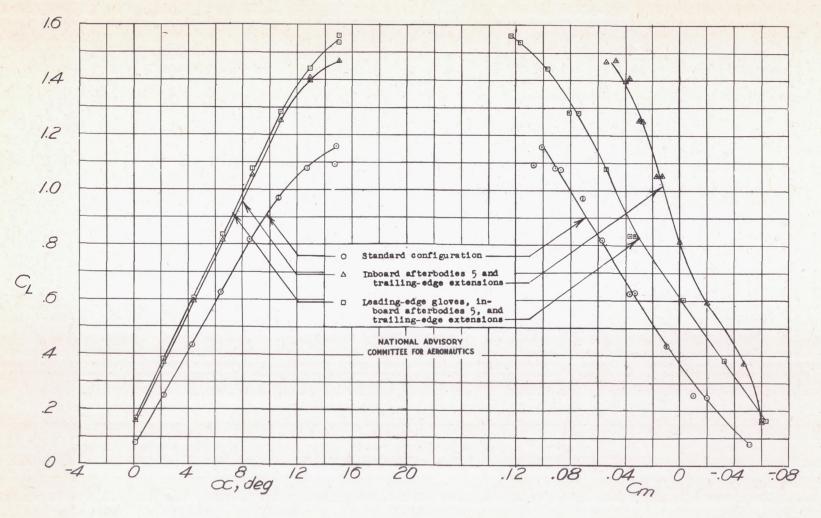


(a) $T_c = 0$.

Figure 54.- Effect of modifications on pitching moment and lift. δ_f = 40°; cowl and intercooler flaps closed; horizontal tail on; transition fixed; R \approx 2,600,000.

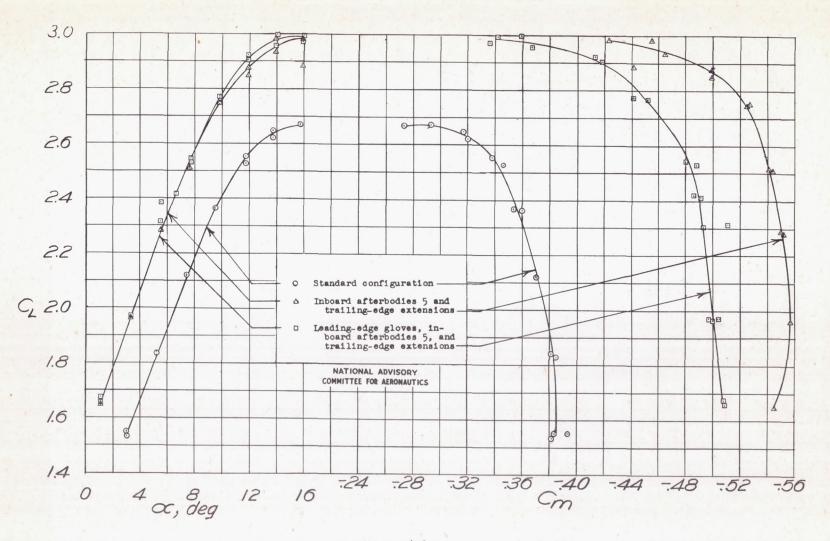


(b) Propellers operating at 0.4 normal rated power. Figure 54. - Concluded.



(a) $\delta_{f} = 09$.

Figure 55.- Effect of modifications on pitching moment and lift. Propellers operating at 0.4 normal rated power; cowl and intercooler flaps closed; horizontal tail off; transition fixed; $R \approx 2,600,000$.



(b) of = 400

Figure 55 .- Concluded.